



Deleterious Variation in BR Serine/Threonine Kinase 2 Classified a Subtype of Autism

Jingxin Deng¹, Yi Wang¹, Meixin Hu¹, Jia Lin², Qiang Li², Chunxue Liu^{1*} and Xiu Xu^{1*}

¹ Division of Child Health Care, National Children's Medical Center, Children's Hospital of Fudan University, Shanghai, China,

² Shanghai Key Laboratory of Birth Defect Prevention and Control, NHC Key Laboratory of Neonatal Diseases, Translational Medical Center for Development and Disease, National Children's Medical Center, Institute of Pediatrics, Children's Hospital of Fudan University, Shanghai, China

OPEN ACCESS

Edited by:

Stephan C. F. Neuhauss,
University of Zurich, Switzerland

Reviewed by:

Julia Dallman,
University of Miami, United States

Ronald P. Hart,
Rutgers, The State University
of New Jersey, United States

*Correspondence:

Chunxue Liu
15111240007@fudan.edu.cn
Xiu Xu
xuxiu@shmu.edu.cn

Specialty section:

This article was submitted to
Methods and Model Organisms,
a section of the journal
Frontiers in Molecular Neuroscience

Received: 26 March 2022

Accepted: 19 May 2022

Published: 10 June 2022

Citation:

Deng J, Wang Y, Hu M, Lin J,
Li Q, Liu C and Xu X (2022)
Deleterious Variation in BR
Serine/Threonine Kinase 2 Classified
a Subtype of Autism.
Front. Mol. Neurosci. 15:904935.
doi: 10.3389/fnmol.2022.904935

Recently, deleterious variants in the BR serine/threonine kinase 2 (*BRSK2*) gene have been reported in patients with autism spectrum disorder (ASD), suggesting that *BRSK2* is a new high-confidence ASD risk gene, which presents an opportunity to understand the underlying neuropathological mechanisms of ASD. In this study, we performed clinical and neurobehavioral evaluations of a proband with a *de novo* non-sense variant in *BRSK2* (p.R222X) with other reported *BRSK2* mutant patients. To validate *BRSK2* as an ASD risk gene, we generated a novel *brsk2b*-deficient zebrafish line through CRISPR/Cas9 and characterized its morphological and neurobehavioral features as well as performed molecular analysis of neurogenesis-related markers. The proband displayed typical ASD behaviors and language and motor delay, which were similar to other published *BRSK2* mutant patients. Morphologically, *brsk2b*^{-/-} larvae exhibited a higher embryonic mortality and rate of pericardium edema, severe developmental delay, and depigmentation as well as growth retardation in the early developmental stage. Behaviorally, *brsk2b*^{-/-} zebrafish displayed significantly decreased activity in open field tests and enhanced anxiety levels in light/dark tests and thigmotaxis analysis. Specifically, *brsk2b*^{-/-} zebrafish showed a prominent reduction of social interaction with peers and disrupted social cohesion among homogeneous groups. Molecularly, the mRNA expression levels of *homer1b* (a postsynaptic density scaffolding protein), and *mbpa*, *mpz*, and *plp1b* (molecular markers of oligodendrocytes and myelination) were increased in the brain tissues of adult *brsk2b*^{-/-} zebrafish, while the expression level of *isl1a*, a marker of motor neurons, was decreased. Taken together, for the first time, we established a novel *brsk2b*-deficient zebrafish model that showed prominent ASD-like behaviors. In addition, the disturbed mRNA expression levels of neurogenesis-related markers implied that the processes of postsynaptic signaling as well as oligodendrocytes and myelination may be involved. This discovery may suggest a path for further research to identify the underlying neuropathological mechanisms between *BRSK2* and ASD.

Keywords: *BRSK2* gene, autism spectrum disorder, zebrafish, neurodevelopment, social preference, animal model

INTRODUCTION

Autism spectrum disorder (ASD) is a heterogeneous neurodevelopmental disorder manifesting in early development that is characterized by persistent deficits in social interaction and restricted, repetitive, or unusual sensory–motor behaviors (Lord et al., 2020). Dozens of cohort studies have elucidated that the heritability of ASD is estimated to range from 60 to 90% (Tick et al., 2016; Bai et al., 2019; Hansen et al., 2019; Castelbaum et al., 2020). Sibling studies have indicated that the risk of ASD occurrence of a subsequent child following an older child with ASD is 8.4-fold higher compared to the risk in unaffected families (Hansen et al., 2019), supporting a strong genetic contribution to ASD pathogenesis. So far, over 100 genetic loci and rare genetic variants have been identified to contribute to ASD (Ronemus et al., 2014; Satterstrom et al., 2020). Identifying additional risk genes associated with ASD will provide pathological insight into our understanding of ASD etiology.

Recently, a novel gene, BR serine/threonine kinase 2 (*BRSK2*, NC_000011.10), was identified as a high-confidence ASD risk gene (Feliciano et al., 2019). A study reported nine patients with rare, heterozygous variants in *BRSK2* from cohorts including 3,429 probands with developmental delay/intellectual disability (DD/ID). Six of the variants were loss-of-function and three were predicted to be damaging missense variants. In particular, 78% (7/9) patients were diagnosed with ASD (Hiatt et al., 2019). Another study (Feliciano et al., 2019) that assessed whole-exome sequencing and genotyping data of 457 autism families provided statistical support for 26 ASD risk genes at a false discovery rate of 0.1 in the SPARK cohort of ASD families. Importantly, among these genes, *BRSK2* is the only one with multiple *de novo*, likely gene-disrupting variants that reached genome-wide significance supporting *BRSK2* as a novel risk gene for ASD. Also known as *SAD1* or *SADA*, *BRSK2* is located at 11p15.5 and is exclusively expressed in the human central nervous system and pancreas. Along with its homolog *BRSK1* (also known as *SAD2* or *SAD-B*, NP_115806.1), the *BRSK2* (NP_001243556.1) protein belongs to the AMPK-related family of protein kinases and plays a role in axon specification and arborization by regulating microtubule dynamics through the phosphorylation of Tau after being phosphorylated by LKB1 (Kishi et al., 2005; Barnes et al., 2007). In addition, *BRSK* kinases have also been demonstrated to localize to synapses and regulate their maturation in the peripheral and central nervous systems (Lilley et al., 2014).

Previous rodent models have been applied to study the molecular mechanisms underlying the neurodevelopmental effects of *BRSK2* and these models displayed some of the phenotypes seen in patients. *Brsk1/Brsk2* null mutant mice displayed neurodevelopmental disruptions including severe dyskinesia and lethality within 2 h after birth as well as a morphologically aberrant thin cortex and disturbed specification of axons and dendrites (Kishi et al., 2005; Dhumale et al., 2018). Since the *Brsk1/Brsk2* mutant mice died perinatally, several conditional knockout mice were also generated. The *BRSK* kinases were both deleted from motor neurons by embryonic day 13.5 in *Brsk^{Isl1-cre}* mice and 15.5 in *Brsk^{ChAT-cre}* mice, respectively. The former

died within 24 h after birth, and the latter survived until adulthood but exhibited mild postural tremors. However, *Brsk2*-single mutant mice were observed to have affected neuronal migration and died several days after birth, which was not replicated in *Brsk1* mutant mice, indicating that *BRSK2*, rather than *BRSK1*, is required for cortical development (Nakanishi et al., 2019). Another *Brsk2*-single knockout mouse developed normally without gross abnormalities, but they exhibited growth retardation and hypoinsulinemia, suggesting impaired islet β -cell function (Nie et al., 2013). Nonetheless, neurobehavioral analyses were insufficient to further study phenotype-genotype correlations when *BRSK2* dysfunction was generated in these rodent models.

In conclusion, although growing evidence indicates that *BRSK2* plays an important role in neurodevelopment, and mutations in the *BRSK2* gene associate with ASD, none of these studies provided direct evidence to illustrate that *BRSK2* dysfunction is relevant to ASD on the basis of ASD animal models. About 60% of human ASD risk genes have orthologs in the zebrafish genome (Meshalkina et al., 2018), and the brain regions of the “social decision-making network” remain largely conserved between mammals and zebrafish (Geng and Peterson, 2019). Thus, zebrafish can be used to model the physiological functions of the human brain and have become a valuable model organism for studying social neurobiology and developmental diseases (Sakai et al., 2018; Rea and Van Raay, 2020).

In this study, we investigated the phenotype-genotype correlations of *BRSK2* mutant patients, and for the first time, we modeled a novel *brsk2*-deficient zebrafish line to analyze the developmental characteristics and neurobehavioral features relevant to ASD.

MATERIALS AND METHODS

Laboratory Animals and Feeding Conditions

The wild-type zebrafish of TU strains were housed in the Institute of Zebrafish, Children’s Hospital of Fudan University. Both larval and adult zebrafish were maintained in standard laboratory conditions: a circulating water system at 28.5°C constant temperature and exposed to a 14-h-light/10-h-dark circadian cycle. All animal experiments were conducted in accordance with the Guiding Principles for the Care and Use of Laboratory Animals and approved by the institutional animal care committee of Children’s Hospital of Fudan University.

Phylogenetic Tree and Comparative Genomics Analysis of BR Serine/Threonine Kinase 2 Gene

The human *BRSK2* gene duplicates into two orthologs, *brsk2a* (NC_007136.7) and *brsk2b* (NC_007118.7) in zebrafish. The nucleotide sequences, amino acid sequences and conserved domains of human *BRSK2* (NP_001243556.1, 736aa), zebrafish *brsk2a* (XP_017209740.1, 873aa) and *brsk2b* (XP_009301703.1, 827aa) were obtained in the national

center for biotechnology information (NCBI) gene database¹ and were aligned for conservation and homology using the DNAMAN software (version 9.0.1.116). Sequences of BRSK2 proteins in ten species were identified using the NCBI blast program and confirmed by the best reciprocal blast (*Homo sapiens*: NP_001243556.1, *Sus scrofa*: XP_020938244.1, *Pteropus vampyrus*: XP_023381426.1, *Mus musculus*: NP_001009929.1, *Anolis carolinensis*: XP_016848950.1, *Danio rerio* brsk2a: XP_017209740.1, *Danio rerio* brsk2b: XP_009301703.1, *Xenopus tropicalis*: XP_004913521.1, *Penaeus monodon*: XP_037797337.1, *Apis mellifera*: XP_006557814.2, *Caenorhabditis elegans*: NP_001076761.1, **Figure 1B**). Multiple alignments were performed and the phylogenetic tree of ten

species were further conducted using MEGA 11 software by the neighbor-joining method.

Generation of *brsk2b* Mutant Zebrafish

The *brsk2b* mutant zebrafish were generated using a CRISPR/cas9 system as previously reported (Albadri et al., 2017). The site-specific guide RNA (gRNA) of *brsk2b* was designed to target exon 4 (target site: 5'-GGGCAGGTTAACACCCAAAG-3') (**Figure 2A** and **Supplementary Table 1**) and synthesized by *in vitro* transcription (MAXIscript™ T7 kit AM1314M, Invitrogen). 600 pg cas9 Nuclease (EnGen™ spy cas9 NLS #M0646, New England Biolabs) and 150 pg gRNA were mixed together and microinjected into one-cell stage of fertilized wild-type zebrafish embryos (F0). Injected embryos were allowed to

¹<http://www.ncbi.nlm.nih.gov/gene/>

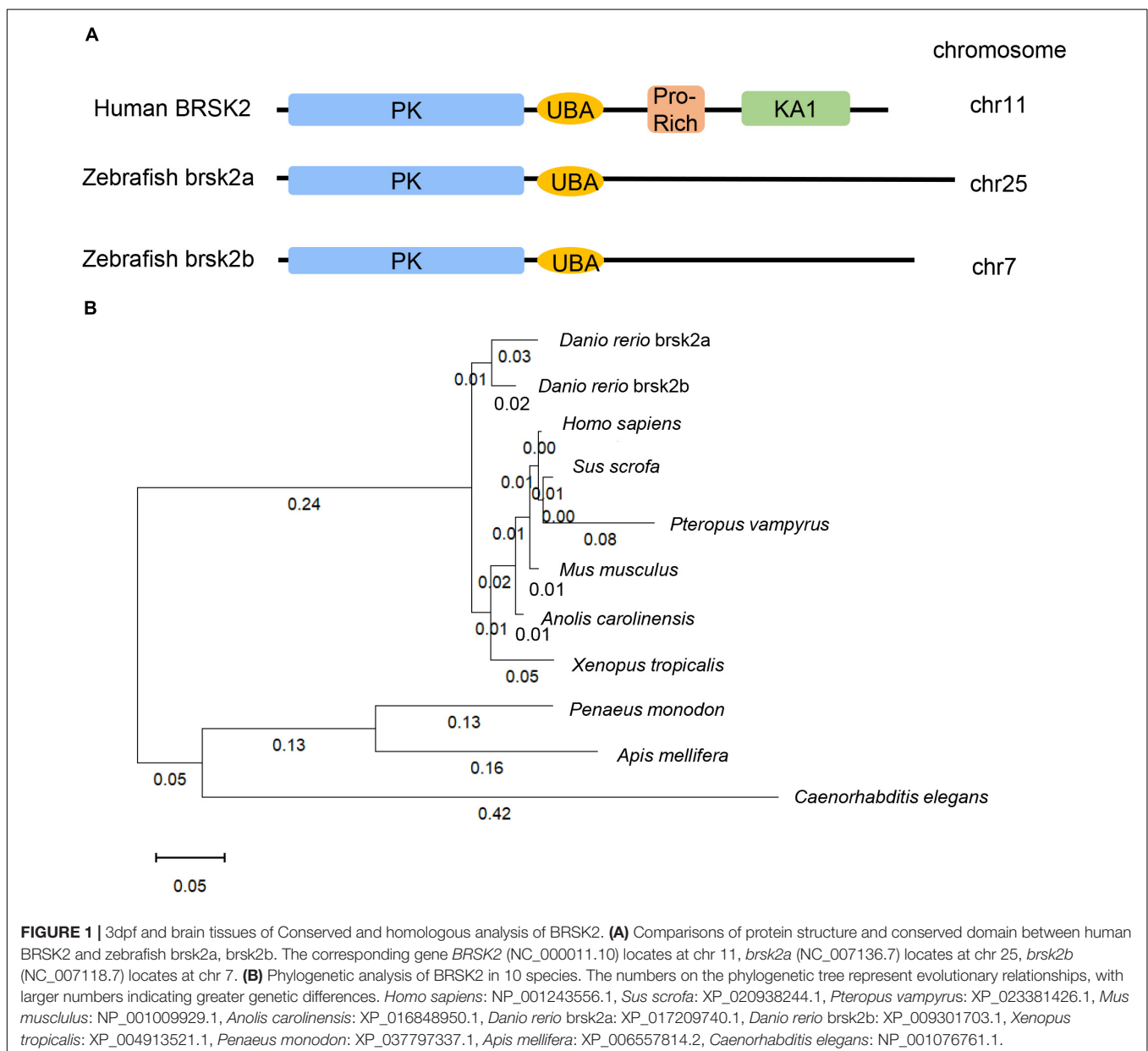
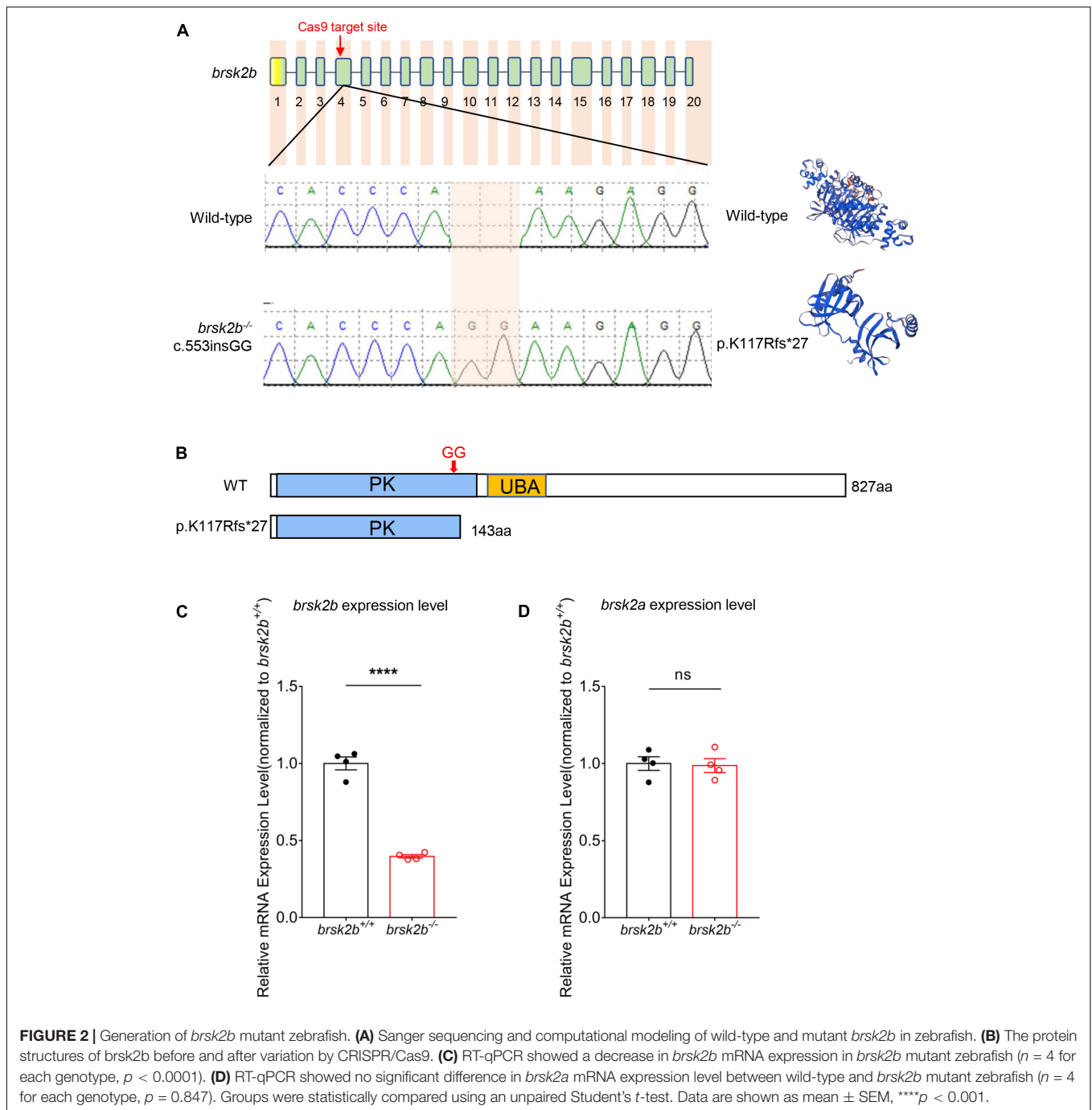


FIGURE 1 | 3dcpf and brain tissues of Conserved and homologous analysis of BRSK2. **(A)** Comparisons of protein structure and conserved domain between human BRSK2 and zebrafish brsk2a, brsk2b. The corresponding gene *BRSK2* (NC_000011.10) locates at chr 11, *brsk2a* (NC_007136.7) locates at chr 25, *brsk2b* (NC_007118.7) locates at chr 7. **(B)** Phylogenetic analysis of BRSK2 in 10 species. The numbers on the phylogenetic tree represent evolutionary relationships, with larger numbers indicating greater genetic differences. *Homo sapiens*: NP_001243556.1, *Sus scrofa*: XP_020938244.1, *Pteropus vampyrus*: XP_023381426.1, *Mus musculus*: NP_001009929.1, *Anolis carolinensis*: XP_016848950.1, *Danio rerio* brsk2a: XP_017209740.1, *Danio rerio* brsk2b: XP_009301703.1, *Xenopus tropicalis*: XP_004913521.1, *Penaeus monodon*: XP_037797337.1, *Apis mellifera*: XP_006557814.2, *Caenorhabditis elegans*: NP_001076761.1.



develop to 72 h post fertilization (hpf), and then 12–20 injected embryos were randomly selected to extract genomic DNA to screen for mutations by PCR amplification and subsequent sanger sequencing. The genotyping PCR amplification conditions were as follows: 95°C, 4 min; 35 cycles of 95°C, 30 s; 58°C, 30 s; 72°C, 45 s; 72°C, 7 min (PCR primers are listed in **Supplementary Table 1**). F0 adult zebrafish were genotyped and crossbred with wild-type zebrafish for at least two generations to select F2 *brsk2b* heterozygous zebrafish, and then F2 fish were in-crossed to obtain homozygous mutants. The SWISS-MODEL

tool² was used to model and visualize the mutant and wild-type protein structures.

Tg (*HuC*: RFP); *brsk2b*^{-/-} Transgenic Zebrafish Maintenance and Imaging

The Tg (*HuC*: RFP) transgenic line was kindly provided by Dr. Xu Wang (Fudan University), which was generated as previously described (Liu et al., 2018). We crossed *brsk2b*

²<https://swissmodel.expasy.org/>

homozygous mutants with Tg (*HuC*: RFP) line to obtain Tg (*HuC*: RFP); *brsk2b*^{-/-} transgenic zebrafish for imaging experiments. Larvae were anesthetized with tricaine at a concentration of 40 mg/L and then viewed on a Leica M205 FA fluorescence microscope at 1, 2, 3 days post fertilization (dpf). In order to maintain the comparative intensities of the fluorescence and not to introduce bias, we used the same settings (Exposure: 6 s, Saturation: 0.9, Gain: 1X, Gamma: 0.8) for all controls and Tg (*HuC*: RFP); *brsk2b*^{-/-} transgenic animals per experiment. Images were taken with no auto-correction to prevent inconsistencies in fluorescence intensity and then were processed using ImageJ software.

RNA Extraction, Reverse Transcription and RT-qPCR

Total RNA was extracted from zebrafish embryos at 1,2,3 dpf and brains at 5,7,10 dpf and 1,3,4 months post fertilization (mpf) using MiniBEST Universal RNA Extraction kit (No.9767, Takara, Japan), according to the manufacturer's protocol. Each condition included 3–4 samples consisting of 20–30 embryos/larvae or 3–4 adult brains per sample for RNA extraction and experiments were conducted in triplicate. Reverse transcription was performed with a PrimeScript™ superscript RT Reagent Kit (RR036Q, Takara, Japan), following the manufacturer's instruction. RT-qPCR was performed using a LightCycler® 480 apparatus (Roche, Germany) and TB Green Premix Ex Taq II (Tli RNaseH Plus) (RR820A, Takara, Japan) to test the mRNA expression levels of *brsk2a*, *brsk2b*, *homer1b*, *nrgna*, *isl1a*, *sox2*, *neurog1*, *olig1*, *olig2*, *sox10*, *mpba*, *mpz*, *plp1b*, according to the manufacturers' protocol. β -actin was chosen as an internal control to normalize the expression levels of target genes by using the delta CT method. The primer sequences for RT-qPCR are listed in Supplementary Table 1.

Morphological Characteristics of *brsk2b* Mutant Zebrafish

To measure the morphological characteristics of *brsk2b* mutant zebrafish, the mortality and rate of pericardium edema, severe developmental delay and depigmentation were calculated at 1 dpf, 2 dpf, and 3 dpf. In addition, the larvae were taken pictures at 1 dpf, 2 dpf, 3 dpf, and 5 dpf laterally or dorsally on a stereo light microscope (Leica M205 FA, United States) after anesthetized with tricaine at a concentration of 40 mg/L (Figure 3A). Then the body length was measured as the distance between the farthest most left and right of the larvae (Figure 3B). Measurements of optic tectum (OT) were also performed as the brain width directly behind the eyes in the dorsal view following previously study (Colón-Rodríguez et al., 2020; Figure 3B). All the measurements were conducted using ImageJ software.

Larval Locomotor Activity and Light/Dark Tests

The locomotor activity of larval zebrafish at 5 dpf was analyzed by a ViewPoint setup combined with an automated computer

recording system equipped with VideoTrack software. The videos were captured with a Point Gray black-and-white camera and recorded for 45 min at 25 fps. The detection threshold was set to 25. Every larva was habituated separately in 24-well plates for 15 min in the experimental chamber before video acquisition. After the former 15-min light period of general locomotor activity, the larvae experienced three dark/light cycles (5 min of dark and 5 min of light per cycle, indicated as D1, L1, D2, L2, D3, L3 in Figures 4A,B, respectively) during the latter 30 min to detect activities under a series of intermittent light stimulation. The light intensity was 100 lx in the light period and 0 lx in the dark period. The frame rate of the video was set to 25/s. The time and distance of larval activity were recorded every 30 s from transformational visual route of every larval trajectory by Zebralab software. For general activity analysis, locomotor activity was quantified as average distance moved per 30 s during the former 15-min light period. For visual motor response triggered by illumination conversion, the activity change in light/dark period was analyzed as velocity change between 30 s before and after the light was turned off or turned on.

Open Field Tests, Stereotype, and Thigmotaxis Analysis

The locomotor activity of adult zebrafish was tested at 4 mpf in an open field paradigm. Videos were captured in a 30 × 30 × 30 cm opaque tank filled with system water using a suspended camera right above. Each male zebrafish was habituated in the tank for 5 min before the 30-min test. The time and distances were recorded every 30 s from transformational visual route of fish trajectory using Zebralab software.

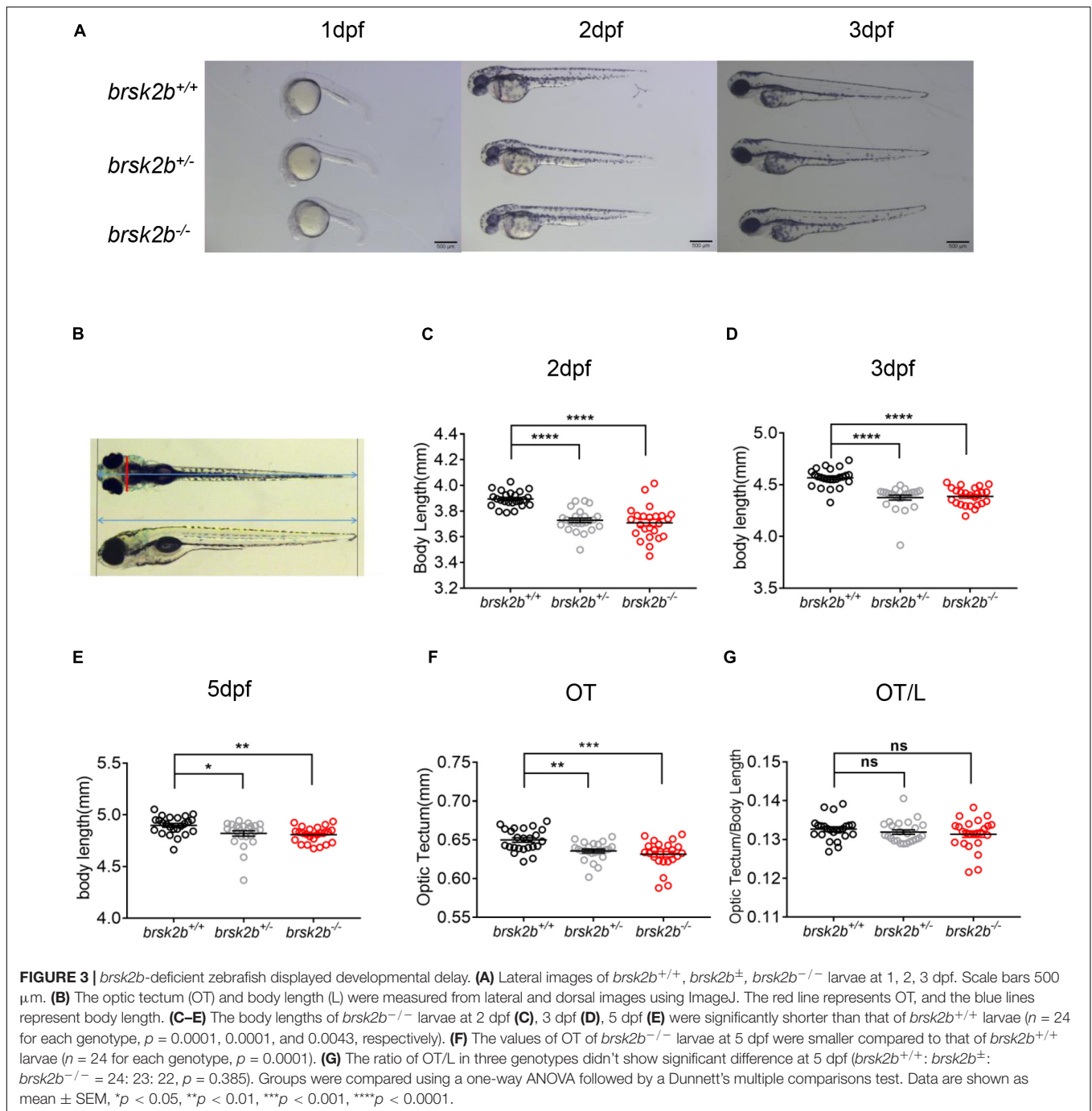
For stereotyped behaviors, double-blind analyses to count the frequency of appearance of the “circling” and “walling” swimming pattern episodes within each minute were conducted separately (Figure 5I).

Thigmotaxis is a well-validated assay for anxiety in adult zebrafish (Kalueff et al., 2013). To analyze thigmotaxis, the open field tank was divided into the peripheral half and the central half (Figure 6E). Then the fish was placed to explore in the tank freely. Thigmotaxis was calculated as the ratio of time or distance that the fish spent in the peripheral zone, which followed the formula below:

$$\text{Thigmotaxis} = \frac{\text{Time/Distance spent in the peripheral zone}}{\text{Time/Distance spent in the whole zone}}$$

Juvenile Zebrafish Social Behavior Tests

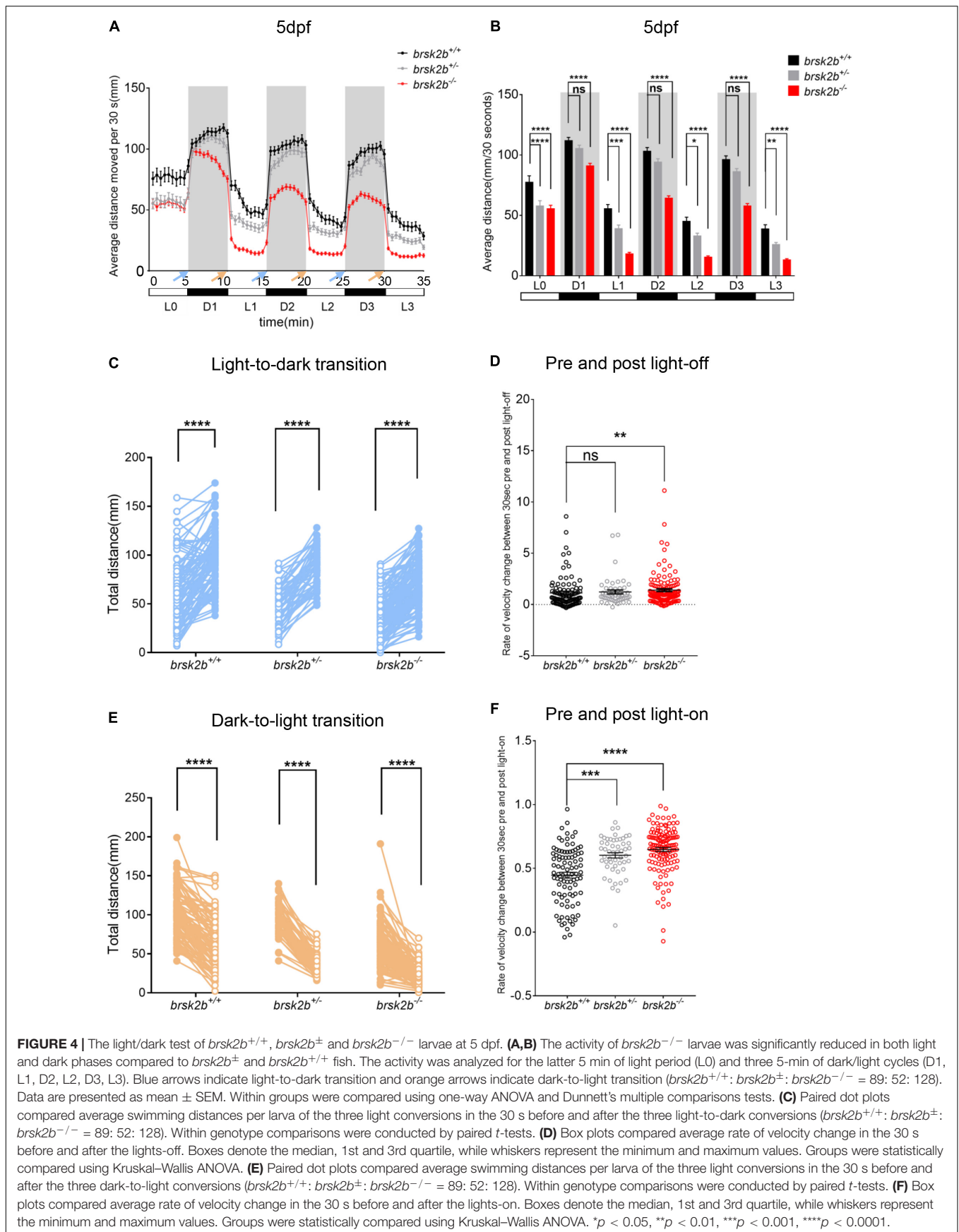
We conducted a social preference test with zebrafish at 1.5 mpf following a previously described experimental paradigm (Ruzzo et al., 2019). The experimental videos were also captured in a ViewPoint setup with automated video tracking system (Viewpoint Life Sciences). The fish were habituated in 12-well plates with removable opaque partitions (Figure 5A). The test fish were placed in the middle row of wells, with one fish per well. A single wild-type conspecific fish of similar age and size was placed in a well either above or below each middle well, with

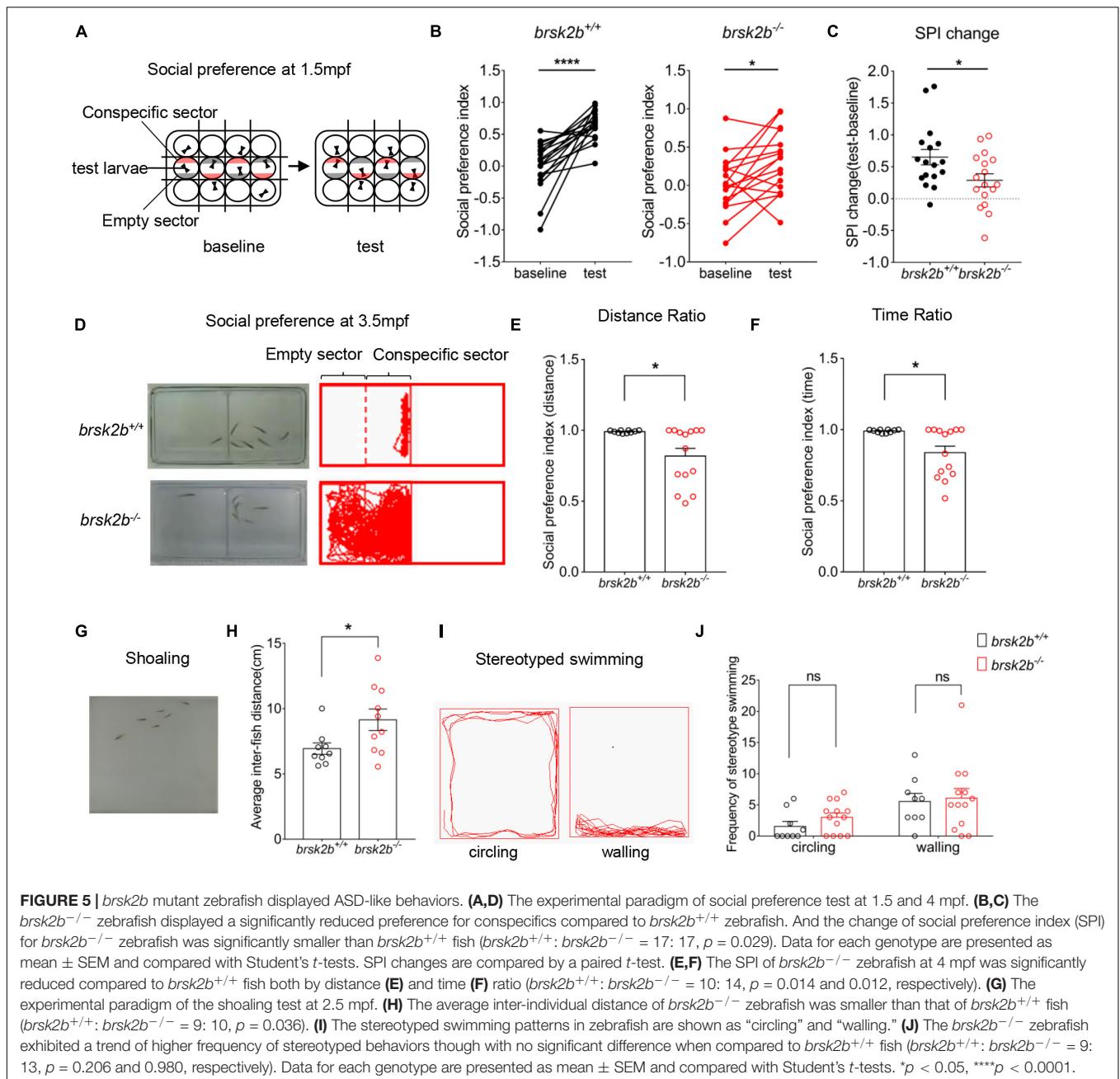


a corresponding opposite well empty. Each assay consisted of 5-min habituation before a 10-min baseline period and another 5-min habituation before a 10-min test period. In the baseline period, opaque partitions were inserted and divided every well to prevent fish from observing each other. Then during the test period, the opaque partitions between each row of wells were removed with the ones between each column of wells remaining, thus the test fish could only see conspecific well and empty well on both sides. When tracking the videos, the time zebrafish spent in both the quarter zone near the conspecific well and

the quarter zone near the empty well was recorded (indicated as conspecific sector and empty sector, respectively, **Figure 5A**). For data analysis, social preference of test fish was measured by calculating the social preference index (SPI), which followed the calculation below:

$$\text{SPI} = \frac{\text{Time spent in conspecific sector} - \text{Time spent in empty sector}}{\text{Time spent in both sectors}}$$





Adult Zebrafish Social Preference Behavior Tests

To further assay social preference of *brsk2b* mutant zebrafish in adulthood, we performed another social experimental paradigm in mating tanks (dimensions 21 × 11 × 7.5 cm). The tank was separated into two equal zones by a transparent divider with a male test fish (wild-type or *brsk2b*^{-/-}) at 3.5 mpf placed in one half and six male wild-type conspecifics of similar size and age placed in another, allowing them to see each other sufficiently **(Figure 5D)**. Fish swam freely for 5-min acclimation before a 30-min video tracking. The time and distance were recorded every 30 s using Zebralab software. When tracking the videos, the half

zone containing test fish was divided into two equal sectors, the conspecific sector close to 6 conspecifics and the empty sector that away from conspecifics **(Figure 5D)**. The social preference was assessed by SPI and calculated as follows:

$$\text{SPI} = \frac{\text{Time/Distance in conspecific sector} - \text{Time/Distance in empty sector}}{\text{Time/Distance in both sectors}}$$

Shoaling Tests

Adult fish form shoaling behavior that they aggregate with each other when swimming in a group of conspecifics. Six

adult male zebrafish of the same genotype (wild-type or *brsk2b*^{-/-}) at 2.5 mpf were placed in the novel tank apparatus for a 5-min habitation before the shoaling test (Figure 5G). Videos tracking fish swimming were recorded for 30 min. The shoaling behavior was quantified as the mean inter-individual distance that indicated the average of all distances between each zebrafish in a group.

Statistical Analysis

Data was analyzed using GraphPad prism software. Normally distributed datasets were compared with the use of Student's *t*-test and one-way ANOVA with Dunnett's multiple comparisons tests. Values were presented as mean ± SEM. Data that were not normally distributed were analyzed as median ± 95% confidence interval using Kruskal–Wallis ANOVA with Dunn's multiple comparisons tests. All statistical tests were 2-tailed, and statistical significance was defined as *p* < 0.05. **p* < 0.05, ***p* < 0.01, ****p* < 0.001, *****p* < 0.0001.

RESULTS

Case Report and Literature Review

The proband was a 7-year-and-6-month-old boy, and first approached the Division of Child Health Care, Children's Hospital of Fudan University at 19 months old due to failure to respond to his name being called. He showed distinct social defects manifesting as use of others' hands as tools, barely responding when directly spoken to, failure to share enjoyment with others, little eye contact or use of body gestures, lack of interest in peers, and preferring solitary activities. Furthermore, he displayed restricted, repetitive patterns of behavior including indulgence in fiddling with round objects, especially wheels, and a narrow range of interest in strings, plastic bags, and neon lights. Moreover, he continued to present problems associated with hypotonia and gastrointestinal problems such as constipation, and had moderate feeding difficulties in the suckling period as reported by his parents.

His birth history was normal in that he was born at 40 weeks gestation and weighed 4,000 g. Due to pathological jaundice after birth, the proband received blue light treatment and stayed in the neonatal ward for 3 days. At the age of 8 months, he began to babble meaningless single syllables but still was not able to speak at first diagnosis. When he was 25 months old, he could only speak a few single words. He also presented motor developmental delay in that he could not walk independently until the age of 18 months. He was first evaluated at 1 year 7 months using the Griffiths Mental Development Scales (locomotor developmental quotient (DQ): 69; personal-social DQ: 46; hearing-speech DQ: 33; hand-eye coordination DQ: 59; performance DQ: 49) (Table 1), indicating global developmental delay. The results of the Autism Diagnostic Observation Schedule (ADOS) were 11 in social affect, 2 in restricted and repetitive behavior, and 13 in total score (ASD cut-off score: 11) (Table 1). Thus, this patient received a diagnosis of ASD based on the DSM-5 criteria and the standardized assessment of ADOS. A brain MRI and EEG showed nothing abnormal. His family history was unremarkable. Genetic

TABLE 1 | Summary of *BRSK2* mutant patients' early development and evaluation results.

Subjects	Our patient	#Patients published
Gender	Male	11/12, Male
Diagnosis of ASD	Yes	10/12, 1/12 Borderline
Speech delay	Yes	12/12
Motor delay	Yes	11/12
Intelligence disability	No	10/12
Age of walking (months)	18	12–20
Age of speaking (months)	25	18–24/non-verbal at evaluation
Comorbidity		
Feeding problem	Yes	2/12
Epilepsy	No	3/12
Sleep disorder	No	3/12
Clinical evaluations		
Age of first GMDS (months)	19.5	–
Locomotor DQ	69	
Personal-social DQ	46	
Hearing-speech DQ	33	
Hand-eye coordination DQ	59	
Performance DQ	49	
Age of WPPSI-IV (years, months)	4.6	–
VCI	88	
VSI	100	
FRI	89	
WMI	76	
PSI	86	
FSIQ	81	
Age of ADOS (months)	19.5	–
Social affect	11	
Restricted and repetitive behavior	2	
Total score	13 (ASD cut-off:11)	

[#]Only 12 of 14 patients with detailed clinical data published in previous studies. GMDS, Griffiths Mental Development Scales. WPPSI-IV, Wechsler Preschool and Primary Scale of Intelligence-Fourth Edition. VCI, Verbal Comprehension Index; VSI, Visual Spatial Index; FRI, Fluid Reasoning Index; WMI, Working Memory Index; PSI, Processing Speed Index; FSIQ, Full Scale Intelligence Quotient. ADOS, Autism Diagnostic Observation Schedule, second edition.

evaluation of exome sequencing revealed a heterozygous non-sense mutation (p.R222X) in *BRSK2*, which leads to a premature translation termination codon and a 221-amino acid truncated protein (Figure 7A). This is a *de novo* variation confirmed by Sanger sequencing of the unaffected parents, and the variant was not found in the ExAC, 1000 Genomes, or ClinVar databases and has not been previously reported in the literature.

Through literature review, we identified 14 other cases with *BRSK2* variants in DD/ID or ASD cohorts (1 microdeletion, 2 non-sense variants, 3 frameshift variants, 4 missense variants, and 5 variants affecting splice sites; Figure 7B). Twelve of the 14 cases reported detailed clinical data (Table 1 and Supplementary Table 2). We compared the phenotypic features of our patient and these 12 cases. Twelve of the 13 cases (92.3%) were male. Their ages ranged from 3 years 8 months to 19 years (mean:

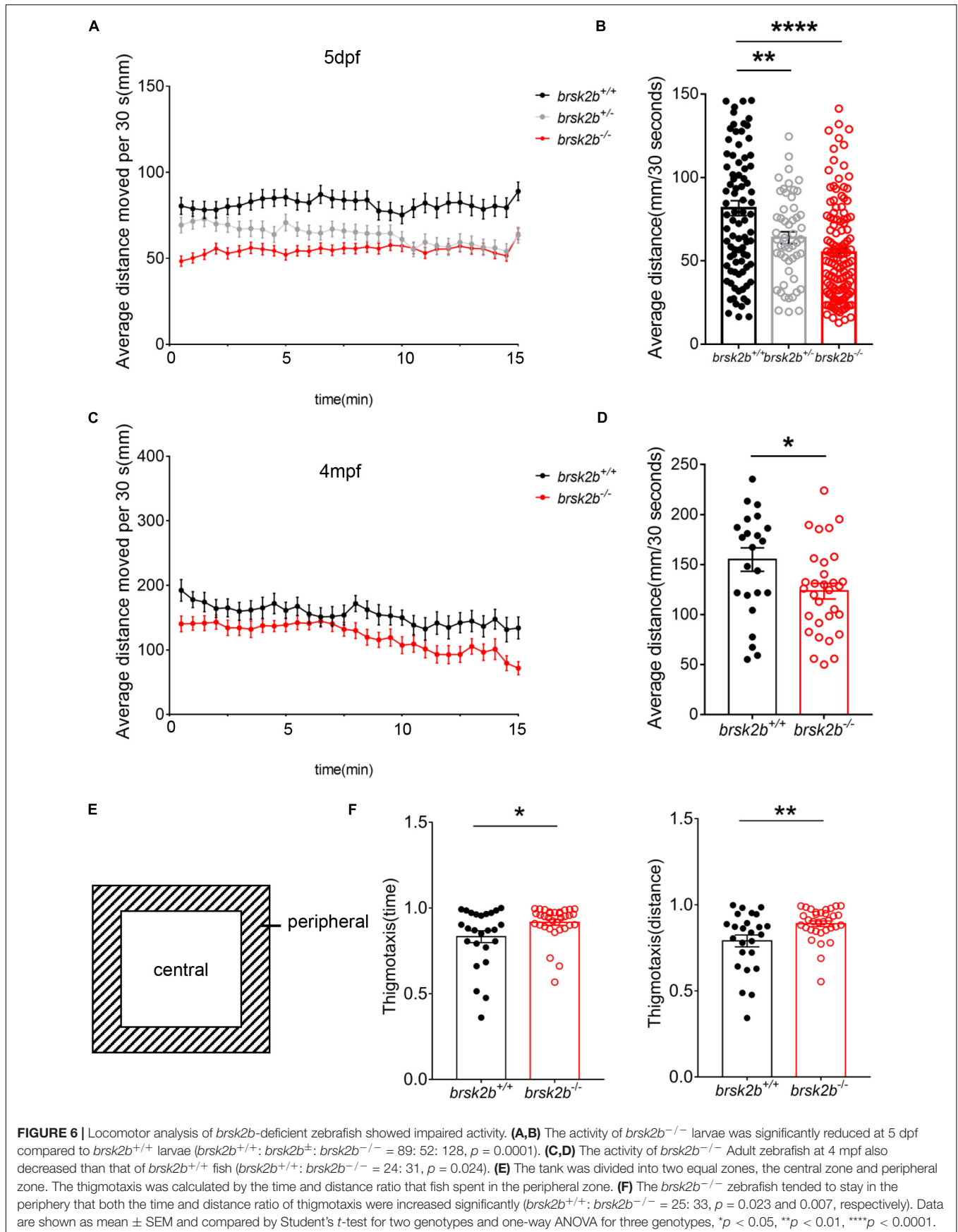
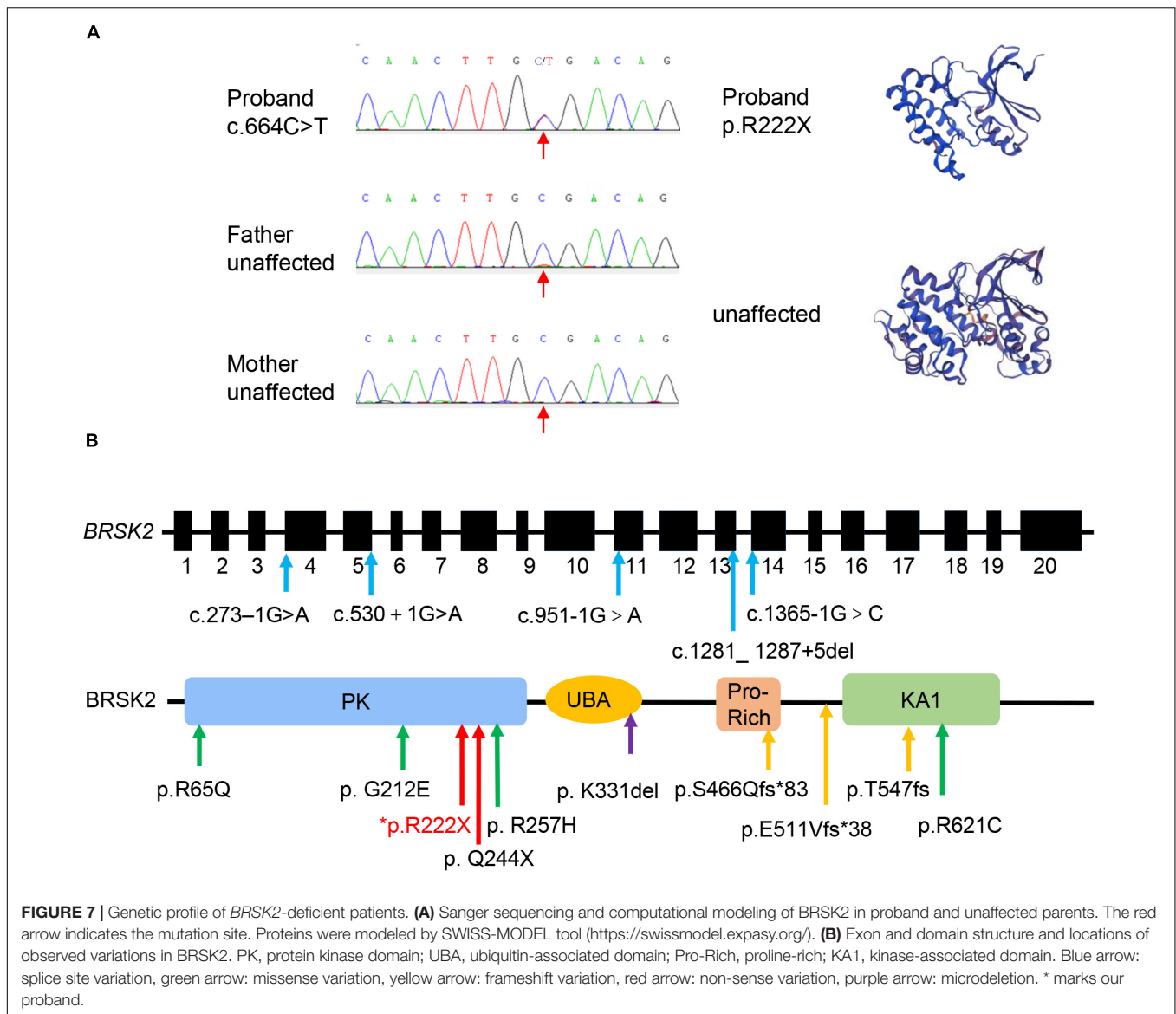


FIGURE 6 | Locomotor analysis of *brsk2b*-deficient zebrafish showed impaired activity. **(A,B)** The activity of *brsk2b*^{-/-} larvae was significantly reduced at 5 dpf compared to *brsk2b*^{+/+} larvae (*brsk2b*^{+/+}: *brsk2b*^{+/-}: *brsk2b*^{-/-} = 89: 52: 128, $p = 0.0001$). **(C,D)** The activity of *brsk2b*^{-/-} Adult zebrafish at 4 mpf also decreased than that of *brsk2b*^{+/+} fish (*brsk2b*^{+/+}: *brsk2b*^{-/-} = 24: 31, $p = 0.024$). **(E)** The tank was divided into two equal zones, the central zone and peripheral zone. The thigmotaxis was calculated by the time and distance ratio that fish spent in the peripheral zone. **(F)** The *brsk2b*^{-/-} zebrafish tended to stay in the periphery that both the time and distance ratio of thigmotaxis were increased significantly (*brsk2b*^{+/+}: *brsk2b*^{-/-} = 25: 33, $p = 0.023$ and 0.007 , respectively). Data are shown as mean \pm SEM and compared by Student's *t*-test for two genotypes and one-way ANOVA for three genotypes, * $p < 0.05$, ** $p < 0.01$, **** $p < 0.0001$.



8 years 5 months; **Supplementary Table 2**). ASD was the most common diagnosis observed in these subjects, with 12 diagnosed (92.3%) and one considered borderline. All patients presented with speech delay (100%, 13/13), 11 presented with motor delay (84.6%, 11/13), and 10 displayed mildly to severely impaired intelligence (76.9%, 10/13). In addition, some were reported to have comorbidities, including sleep disorders (23.1%, 3/13), feeding problems (15.4%, 2/13), and ADHD (23.1%, 3/13) (**Table 1**). Details are presented in **Supplementary Table 2**.

BR Serine/Threonine Kinase 2 Is a Conserved Gene in the Vertebrate Lineage

The zebrafish *brsk2a* gene is located on chromosome 25 and has 20 exons, and the *brsk2b* gene is located on chromosome 7 and has 21 exons (**Figure 1A**). To analyze the evolutionary

conservation of *BRSK2* between human and zebrafish, we performed protein sequence alignments of these two species in detail. The results showed that both the *brsk2a* and *brsk2b* proteins exhibited a high level of amino acid identity with human *BRSK2* (85.47 and 89.59%, respectively; **Table 2**). In particular, the protein kinase domains and UBA domains of both *brsk2a* and *brsk2b* were highly concordant with those of human *BRSK2* (96.41 and 97.13% for the PK domain, and 86.05 and 83.72% for the UBA domain, respectively; **Table 2**). Therefore, zebrafish is a good model for studying the function of the human *BRSK2* protein and its association with ASD.

To further identify orthologs between zebrafish *brsk2* and other species, we built a phylogenetic tree to conduct phylogenetic analysis (**Figure 1B**). The numbers on the phylogenetic tree represent evolutionary relationships, with larger numbers indicating larger genetic differences. In vertebrate animals, the genetic distance was not greater than 0.1; however,

TABLE 2 | Conservation analysis of domains and proteins of BRSK2 between human and zebrafish.

Protein alignment	Conserved level of protein	Conserved level of PK domain	Conserved level of UBA domain
BRSK2 VS. brsk2a	85.47%	96.41%	86.05%
BRSK2 VS. brsk2b	89.59%	97.13%	83.72%
BRSK2A VS. brsk2b	86.78%	97.95%	96.30%

The analysis was performed by DNAMAN software (version 9.0.1.116).

in invertebrates (such as *Caenorhabditis elegans*), the distance was as high as 0.8 (Figure 1B). Therefore, this phylogenetic analysis indicated that *BRSK2* has high evolutionary conservation among vertebrates.

Previous research showed that *Brsk2* is mainly expressed in the cerebrum in rodents (Kishi et al., 2005). To determine the temporal and developmental expression patterns of *brsk2a* and *brsk2b* in zebrafish, RT-qPCR was performed to verify *brsk2* expression levels of wild-type zebrafish at eight developmental stages. The results showed that the expression levels of *brsk2a* and *brsk2b* generally increased with development. Expression of *brsk2a* began at a very early stage (1 dpf) and remained at a relatively low level during the larval period, following a slow increase before reaching its highest level in adulthood (3 mpf) (Figure 8A). The expression level of *brsk2b* was relatively high at 2 dpf, subsequently decreasing at 3 dpf and increasing at 5 dpf, then displayed another increasing peak between 1 mpf and adulthood (Figure 8B). In summary, these data indicate that both *brsk2a* and *brsk2b* are expressed during development and continue to be enriched in the mature central nervous system.

Generation of *brsk2b* Mutant Zebrafish

To determine *BRSK2* function *in vivo*, we generated a loss-of-function variant of *brsk2b* in zebrafish using CRISPR/Cas9 mutagenesis technology (Auer et al., 2014). The *brsk2b*^{-/-} mutant harbors a 2-basepair (GG) insertion resulting in a frameshift mutation and a 143-amino acid truncated protein (Figures 2A,B). RT-qPCR showed that mRNA expression levels of *brsk2b* were dramatically decreased in mutant zebrafish (Figure 2C), while *brsk2b* deficiency did not affect the mRNA expression level of *brsk2a* (Figure 2D). Therefore, these results demonstrate that the *brsk2b* mutant zebrafish line was successfully generated.

The *brsk2b* Mutant Larvae Display Developmental Delay at Early Stages

As previous studies demonstrated that *BRSK2* is essential to early neurogenesis in rodents (Kishi et al., 2005; Nakanishi et al., 2019), we analyzed the morphological characteristics of *brsk2b* mutant zebrafish larvae in early developmental stages (1–3 dpf). Compared with *brsk2b*^{+/+} and *brsk2b*[±] larvae, a significantly larger proportion of *brsk2b*^{-/-} larvae died at 24 hpf (65.9%) and manifested pericardium edema, severe developmental delay, and depigmentation at 48 hpf (26.1%) and 72 hpf (9.1%) (Table 3). The *brsk2b*^{-/-} and *brsk2b*[±] larvae

displayed much shorter body lengths than *brsk2b*^{+/+} larvae at 2 dpf (*brsk2b*^{+/+}: 3.869 ± 0.06 mm; *brsk2b*[±]: 3.728 ± 0.09 mm; *brsk2b*^{-/-}: 3.709 ± 0.13 mm, *p* < 0.0001), 3 dpf (*brsk2b*^{+/+}: 4.567 ± 0.09 mm; *brsk2b*[±]: 4.376 ± 0.12 mm; *brsk2b*^{-/-}: 4.387 ± 0.09 mm, *p* < 0.0001), and 5 dpf (*brsk2b*^{+/+}: 4.899 ± 0.09 mm; *brsk2b*[±]: 4.820 ± 0.13 mm; *brsk2b*^{-/-}: 4.808 ± 0.08 mm, *p* = 0.0043 and 0.0145, respectively), which indicated a pattern of growth retardation (Figures 3C–E). We also measured the value of OT, which is correlated with width of the head, and found that *brsk2b*[±] and *brsk2b*^{-/-} larvae exhibited smaller OT at 5 dpf compared to *brsk2b*^{+/+} larvae (*brsk2b*^{+/+}: 0.650 ± 0.01 mm; *brsk2b*[±]: 0.636 ± 0.01 mm; *brsk2b*^{-/-}: 0.632 ± 0.02 mm, *p* = 0.0028 and 0.00001, respectively; Figure 3F). However, there was no significant difference of the ratio of OT/body length among the three lines (*brsk2b*^{+/+}: 0.133 ± 0.002; *brsk2b*[±]: 0.132 ± 0.003; *brsk2b*^{-/-}: 0.131 ± 0.004, *p* = 0.648 and 0.287, respectively; Figure 3G).

brsk2b Mutant Zebrafish Exhibit Impaired Locomotor Activity in Both the Larval Phase and Adulthood

As most *BRSK2* mutant patients show motor delays, locomotor activity was measured in both the larval and adult zebrafish. During the 15-min observation, the larvae at 5 dpf displayed a significant decrease in the average swimming velocity of *brsk2b*^{-/-} zebrafish (54.86 ± 29.48 mm/30 s) and *brsk2b*[±] zebrafish (63.80 ± 25.81 mm/30 s) compared to *brsk2b*^{+/+} zebrafish (81.52 ± 42.07 mm/30 s, *p* = 0.0001 and 0.0053, respectively; Figures 6A,B). Similarly, a significantly reduced swimming velocity was observed in *brsk2b*^{-/-} fish at 4 mpf compared with *brsk2b*^{+/+} fish (*brsk2b*^{-/-} vs. *brsk2b*^{+/+}: 123.4 ± 43.64 mm/30 s vs. 155.0 ± 57.29 mm/30 s, *p* = 0.0241; Figures 6C,D). Moreover, *brsk2b*^{-/-} zebrafish showed steadily lower locomotor activity throughout the examination window.

In the analysis of the light/dark test, the average swimming distance of *brsk2b*^{-/-} larvae during each 5-min light or dark period was dramatically lower (D1: 90.91 ± 25.056 mm/30 s, *p* < 0.0001; L1: 18.144 ± 15.271 mm/30 s, *p* < 0.0001; D2: 64.259 ± 22.252 mm/30 s, *p* < 0.0001; L2: 15.318 ± 13.194 mm/30 s, *p* < 0.0001; D3: 57.902 ± 21.509 mm/30 s, *p* < 0.0001, L3: 13.126 ± 12.103 mm/s, *p* < 0.0001; Figures 4A,B) than *brsk2b*^{+/+} and *brsk2b*[±] larvae, which provides additional evidence of impaired locomotor phenotypes in *brsk2b*^{-/-} fish.

We also examined the responses evoked by light-dark switching. In general, light-to-dark transitions elicit sudden increases in swimming velocity, while dark-to-light transitions result in sudden decreased velocity, which is called the visual motor response (Burton et al., 2017). As reported, a sudden increase evoked by the illumination conversion was used to represent the anxiety level of the zebrafish (Krylov et al., 2021). During three light-to-dark transitions, the *brsk2b*^{-/-} zebrafish at 5 dpf exhibited a trend of enhanced movement with a higher velocity change compared to the other lines [*brsk2b*^{+/+}: 0.62 (95% CI: 0.816–1.451); *brsk2b*[±]: 0.82 (95% CI: 0.840–1.605); *brsk2b*^{-/-}: 1.01 (95% CI: 1.13–1.67); Figures 4C,D] during the

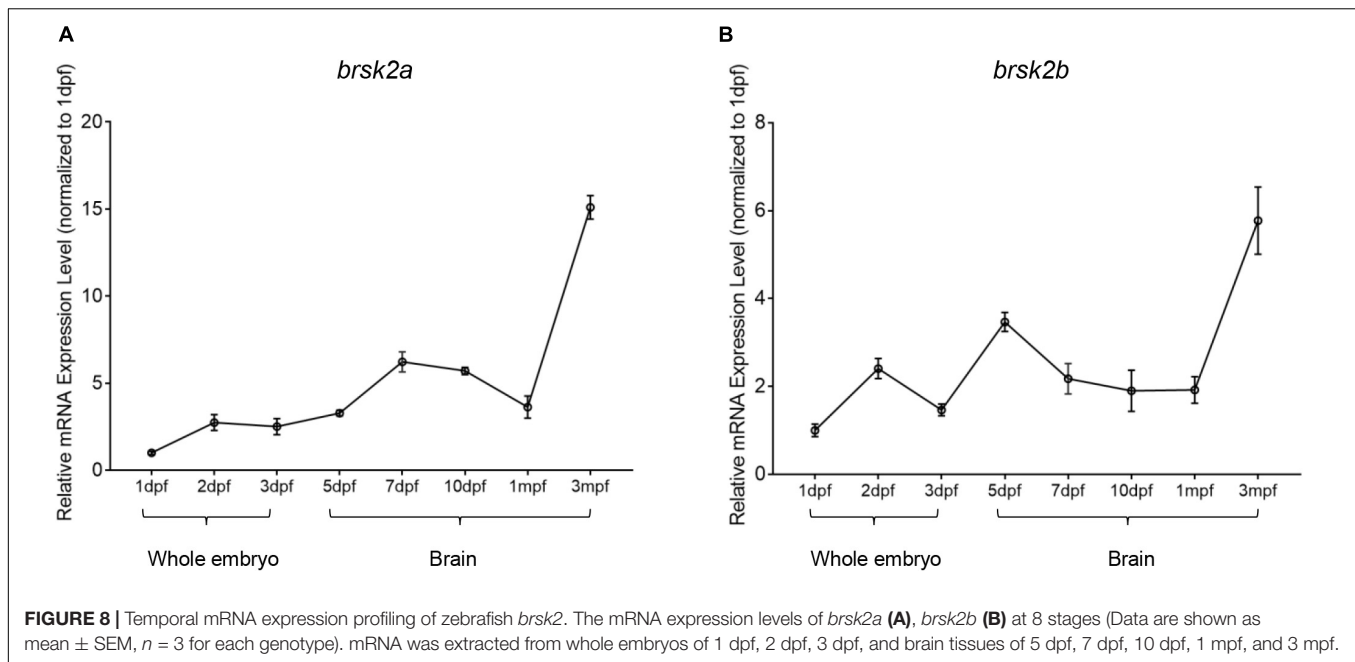


TABLE 3 | Mortality and morphological analysis in early development.

	<i>brsk2b</i> ^{+/+}	<i>brsk2b</i> ^{+/-}	<i>brsk2b</i> ^{-/-}
Mortality at 24 hpf	2/92 (2.2%)	8/59 (13.6%)	54/82 (65.9%)
#Abnormal development at 48 hpf	0/30 (0%)	5/27 (18.5%)	6/23 (26.1%)
#Abnormal development at 72 hpf	2/40 (5%)	10/47 (21.2%)	2/22 (9.1%)

#Abnormal development includes pericardium edema, severe developmental delay and depigmentation.

30 s before and after the light was turned off. Similarly, in three dark-to-light transitions, the velocity change of *brsk2b*^{-/-} larvae was more dramatic than that of the other lines [*brsk2b*^{+/+}: 0.47 (95% CI: 0.401–0.492); *brsk2b*[±]: 0.60 (95% CI: 0.560–0.644); *brsk2b*^{-/-}: 0.68 (95% CI: 0.616–0.679); **Figures 4E,F**]. Our analysis found that *brsk2b*^{-/-} larvae exhibited a larger velocity change when the lights were turned off and on, which might indicate that *brsk2b*^{-/-} larvae present more stress when illumination changes. In addition, thigmotaxis was also measured in adult zebrafish to analyze anxiety-like behaviors. The results showed that *brsk2b*^{-/-} zebrafish at 4 mpf spent more swimming time and distance in the peripheral zone (0.92 \pm 0.02 for time ratio and 0.89 \pm 0.02 for distance ratio) compared to *brsk2b*^{+/+} zebrafish (0.83 \pm 0.03 for time ratio and 0.79 \pm 0.03 for distance ratio, **Figure 6F**). In summary, our work demonstrates that *brsk2b*^{-/-} zebrafish had higher anxiety.

brsk2b Mutant Zebrafish Display Autism Spectrum Disorder-Like Behaviors

To assay whether *brsk2b* mutant zebrafish displayed ASD-like characteristics, we performed multiple tests of ASD-like behaviors from juvenile to adult zebrafish. We first performed

a modified social preference test on 1.5 mpf juvenile zebrafish (**Figure 5A**). The results showed that *brsk2b*^{+/+} zebrafish generally spent more time in the conspecific sector rather than the empty sector, implicating a strong group tendency. In contrast, *brsk2b*^{-/-} fish exhibited a reduced duration and frequency of social contact with peer wild-type fish, and their SPI change between the baseline period and the test period was significantly decreased compared to *brsk2b*^{+/+} zebrafish, indicating that juvenile *brsk2b*^{-/-} zebrafish showed a significant social deficit (**Figures 5B,C**). Similarly, in the adult (3.5 mpf) social preference assay, *brsk2b*^{-/-} fish spent their time evenly throughout the region and displayed a reduced duration and frequency of social contact with the peer group compared to *brsk2b*^{+/+} fish, indicating a significantly decreased social preference (**Figures 5E,F**). The shoaling test is another important social behavioral test. In the shoaling assay, *brsk2b*^{+/+} zebrafish tended to aggregate together and showed much smaller inter-fish distances, while the *brsk2b*^{-/-} zebrafish swam more separately and displayed larger and looser schools, as well as much larger inter-fish distances (**Figure 5H**). The analysis of trajectories of activity and patterns of swimming showed that *brsk2b*^{-/-} zebrafish exhibited a trend of a higher frequency of stereotyped behaviors, although they were not significantly different to *brsk2b*^{+/+} fish (**Figure 5J**).

brsk2b Disruption Affects Normal Neurodevelopment in Mutant Zebrafish

To identify potential mechanisms underlying ASD-like behaviors, we first assessed the impact of neurodevelopment *in vivo*, as a previous study observed that *Brsk1/Brsk2* double mutant mice displayed aberrant cortex development (Kishi et al., 2005). We crossed *brsk2b*^{-/-} zebrafish with a Tg (*HuC*: RFP) transgenic line in which RFP protein expression is

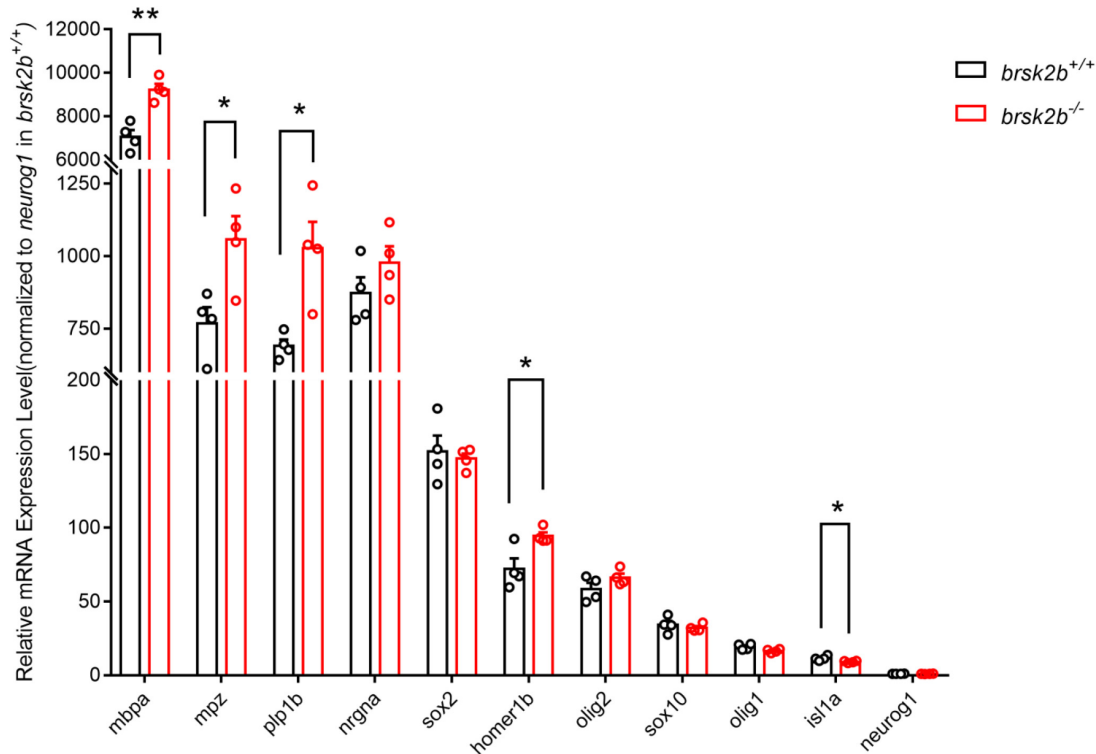


FIGURE 9 | RT-qPCR showed altered expression levels of neurogenesis-related markers in *brsk2b*^{-/-} zebrafish. Human homologous protein: HOMER1, Homer Scaffold Protein 1, a postsynaptic density scaffolding protein; NRG1, Neurogranin, a postsynaptic protein kinase substrate; ISL1, a DNA-binding transcriptional activator; SOX2, a transcription factor regulating embryonic development and determining cell fate; NEUROG1, a transcriptional regulator involved in the initiation of neuronal differentiation; OLIG1, Oligodendrocyte Transcription Factor 1, promotes formation and maturation of oligodendrocytes; OLIG2, Oligodendrocyte Transcription Factor 2, required for oligodendrocyte and motor neuron specification in the spinal cord; SOX10, a transcription factor that plays a central role in developing and mature glia; MBP, a major constituent of the myelin sheath of oligodendrocytes and Schwann cells in the nervous system; MPZ, a major structural protein of the peripheral myelin sheath; PLP, a major myelin protein in central nervous system. $n = 4$ for each genotype, data for each gene are shown as mean \pm SEM and compared with multiple t -tests. * $p < 0.05$, ** $p < 0.01$.

specifically controlled by the neural *HuC* promoter, allowing the visualization of neurodevelopment at embryonic stages. As shown in **Supplementary Figure 1**, the RFP signal intensities of *brsk2b*^{-/-} larvae at 1, 2, and 3 dpf were dramatically decreased compared to *brsk2b*^{+/+} larvae, indicating a deleterious effect on neurodevelopment.

In addition, we examined the mRNA expression levels of a group of markers involved in neurogenesis, including a postsynaptic density scaffolding protein (*homer1b*), general neurogenesis proteins (*nrgna*, *neurog1*, and *sox2*), a motor neuron-specific protein (*isl1a*), and oligodendrocyte-related proteins (*olig1*, *olig2*, *sox10*, *mbpa*, *mpz*, and *plp1b*). When normalized to the expression level of *neurog1* in wild-type zebrafish, the results showed that the mRNA expression levels of *homer1b* (*brsk2b*^{+/+}: *brsk2b*^{-/-} = 72.17 ± 7.082 : 94.41 ± 2.547 , $p = 0.025$), *mbpa* (*brsk2b*^{+/+}: *brsk2b*^{-/-} = $7,064 \pm 317.6$: $9,229 \pm 265.7$, $p = 0.002$), *mpz* (*brsk2b*^{+/+}: *brsk2b*^{-/-} = 768.8 ± 55.54 : $1,058 \pm 80.27$, $p = 0.025$), and *plp1b* (*brsk2b*^{+/+}: *brsk2b*^{-/-} = 691.4 ± 22 : $1,028 \pm 90.76$, $p = 0.011$) in *brsk2b*^{-/-} zebrafish were significantly increased compared to *brsk2b*^{+/+} zebrafish, while the expression level of *isl1a* was clearly decreased

(*brsk2b*^{+/+}: *brsk2b*^{-/-} = 11.5 ± 0.834 : 9.08 ± 0.345 , $p = 0.037$). Otherwise, no significant differences were observed in the levels of *neurog1* (*brsk2b*^{+/+}: *brsk2b*^{-/-} = 1 ± 0.005 : 0.98 ± 0.068 , $p = 0.794$), *nrgna* (*brsk2b*^{+/+}: *brsk2b*^{-/-} = 873.1 ± 54.31 : 978.5 ± 56.39 , $p = 0.2271$), *sox2* (*brsk2b*^{+/+}: *brsk2b*^{-/-} = 151.7 ± 10.83 : 146.8 ± 3.559 , $p = 0.680$), *olig1* (*brsk2b*^{+/+}: *brsk2b*^{-/-} = 19.31 ± 1.003 : 16.54 ± 0.634 , $p = 0.059$), *olig2* (*brsk2b*^{+/+}: *brsk2b*^{-/-} = 58.48 ± 4.209 : 66.26 ± 2.634 , $p = 0.168$), and *sox10* (*brsk2b*^{+/+}: *brsk2b*^{-/-} = 34.23 ± 2.73 : 32.15 ± 1.223 , $p = 0.514$) (**Figure 9**). These data illustrate that the neurodevelopment of *brsk2b*^{-/-} zebrafish might be affected through disturbed synaptogenesis, oligodendrocyte maturation, and myelin sheath formation.

DISCUSSION

Here, we report a novel *BRSK2* non-sense variant in a patient with ASD. The patient displayed distinct social defects and a narrow range of interests with mild developmental delay in language and motor skills. To determine the correlation between genotype and phenotype, we established *brsk2b* mutant zebrafish with

CRISPR/Cas9 technology. Morphological assessment revealed that *brsk2b* mutant larvae exhibited higher embryonic lethality and rate of pericardium edema, severe developmental delay and depigmentation as well as growth retardation. The *brsk2b* mutant zebrafish displayed ASD-like behaviors and showed locomotor dysfunction in both the juvenile and adult stages. In addition, we found that the mRNA expression level of *homer1b*, *mbpa*, *mpz*, and *plp1b* were increased, while *islla* was decreased in *brsk2b* mutant zebrafish, indicating disrupted postsynaptic structure and oligodendrocyte function. In summary, we conclude that *brsk2b* dysfunction in zebrafish induced early developmental delay and behavioral abnormalities similar to those seen in autism.

The patient in this study was diagnosed with ASD for social defects and manifested speech and motor delays, which were concordant with the symptoms of *BRSK2* patients reported in previously published literature (Feliciano et al., 2019; Hiatt et al., 2019). Exome sequencing data revealed that the patient had a *de novo* non-sense variant in *BRSK2* (p.R222X), which was predicted to be deleterious. Previous publications reported that 14 described non-sense, splice, frameshift, and predicted-deleterious missense *BRSK2* variations were likely responsible for the phenotypes of these DD/ID patients with or without ASD (Miller et al., 2010; Kaminsky et al., 2011; Feliciano et al., 2019; Hiatt et al., 2019). Therefore, these cases indicate that *BRSK2* is relatively intolerant to protein-altering variation and plays a role in neurological diseases including ASD.

BRSK2 is highly evolutionarily conserved in vertebrates, and both the *brsk2a* and *brsk2b* protein in zebrafish exhibit a high level of amino acid identity with human *BRSK2*. A recent study demonstrated that *Brsk2*-deficient mice showed neonatal lethality and a disorganized cortex after being backcrossed with C57BL/6 mice for at least six generations, which was not observed in *Brsk1*-deficient mice, indicating that *Brsk2* plays a more essential role in neurodevelopmental and cortical process in rodents (Nakanishi et al., 2019). In our study, *brsk2b*-deficient zebrafish exhibited a higher embryonic mortality rate and dysplasia including pericardium edema, severe developmental delay, and depigmentation when compared to wild-type zebrafish. Though non-negligible embryonic lethality was observed in some individuals, the *brsk2b*-deficient zebrafish were able to survive to adulthood and were fertile. The duplication of the *brsk2* gene in zebrafish may account for this difference between *Brsk2*-deficient mice and zebrafish in that *brsk2a* may perform similar functions as *brsk2b*. Notwithstanding, our RT-qPCR experiment did not reveal any compensational increase of *brsk2a* mRNA, but we speculate that the function of *brsk2a* was retained after *brsk2b* was defective, which may compensate for some of the phenotypes. Furthermore, *brsk2b*-deficient larvae had shorter body lengths than wild-type larvae at 2, 3, and 5 dpf. This observation was also reminiscent of the growth retardation observed in a *Brsk2* knockout mouse model (Nie et al., 2013). Although the value of OT, representing the brain size of *brsk2b* mutant larvae, was smaller than those of wild-type larvae at 5 dpf, the ratio of OT to body length did not show any difference. Particularly, our observation of weaker RFP signals in the neural system of Tg (*huC*: RFP); *brsk2b* mutant larvae demonstrated

that *brsk2b* dysfunction disturbed neurodevelopment. Previously cultured hippocampal and cortical neurons from *Brsk1/Brsk2* double knockout mice *in vitro* exhibited disrupted polarization and a large proportion of indeterminate neurites, which were positive for both axonal and dendritic markers (Muller et al., 2010; Dhumale et al., 2018). And *Brsk1/Brsk2* double mutant mice showed reduced cortical axon tracts and displayed a much thinner cortex in which the apoptosis of neurons and a reduction of progenitors were detected (Kishi et al., 2005; Dhumale et al., 2018). Together, our observations, which echo findings in rodent animals, provide additional evidence that *brsk2b* dysfunction affects embryonic neurodevelopment.

Locomotion is the most basic and complex motor behavior in vertebrates which is controlled by neural activity (Grillner and El Manira, 2020). Disrupted neural structures and dysregulated brain development may affect the locomotor behavior of zebrafish larvae (Liu et al., 2022). In the activity test, *brsk2b*^{-/-} larvae demonstrated hypoactivity, with their average swimming distance per 30 s being much shorter than that of *brsk2b*[±] and *brsk2b*^{+/+} larvae. This aberrant motor pattern remained during the adult stage, with *brsk2b*^{-/-} zebrafish at 4 months old also displaying lower average movement compared to their wild-type counterparts in open field tests. These discoveries are analogous to patients with *BRSK2* variants in that 84.6% of reported cases (11/13) experienced motor developmental delays at an early age and exhibited motor function impairments thereafter (Feliciano et al., 2019; Hiatt et al., 2019). Although *Brsk2* null mice studies did not show detailed data on behavioral tests (Kishi et al., 2005; Nakanishi et al., 2019), these mice exhibited little spontaneous movement (Kishi et al., 2005), and the neuromuscular junction of conditional *Brsk1/Brsk2* null mice had disorganized neurofilaments and required *BRSK* kinases presynaptically for synaptic maturation (Lilley et al., 2014). Thus, our work suggests that *brsk2* deficiency impairs the motor function of *brsk2b* mutant zebrafish. In addition, further detection of the mRNA level revealed that the expression of *islla*, a motor neuron specific gene, was reduced, which might underlie the motor defects in *brsk2b* mutant fish.

It is known that anxiety is one of the comorbid symptoms in ASD (Meshalkina et al., 2018) and one of the reported patients with *BRSK2* variation (p. Gln244X) was diagnosed with anxiety disorder, so we evaluated whether this phenotype was displayed in *brsk2b* mutant zebrafish in behavioral tests. In nature, the response to the conversion in illumination reflects an aversion of darkness, which is a survival instinct to escape predators casting shadows on zebrafish larvae (Mahabir et al., 2013). Thus, sudden increased activity evoked by light changes reflects a state of stress, and this visual motor response is considered an index of anxiety (Ellis et al., 2012; Schnorr et al., 2012; Peng et al., 2016; Basnet et al., 2019). While all the three genotypes of *brsk2b* larvae at 5 dpf showed sudden increased activity provoked by dark, *brsk2b*^{-/-} larvae exhibited a more remarkable transient velocity change between the 30 s before and after the light-to-dark and dark-to-light transition. Since the average activity of *brsk2b*^{-/-} larvae in both the light and dark phases was lower than that of *brsk2b*[±]

and *brsk2b*^{+/+} larvae, we speculate that *brsk2b*^{-/-} larvae displayed anxiety-like behavior. On the other hand, thigmotaxis is a well-validated index of anxiety that is evolutionarily conserved and is displayed by a wide range of species (Treit and Fundytus, 1988). Thigmotaxis (also called “wall-hugging” or “wall-following” behavior) is the propensity to avoid the center of an arena and stay or move in close proximity to the boundaries of a novel environment (Sharma et al., 2009; Schnorr et al., 2012). In our study, the adult *brsk2b*^{-/-} zebrafish reduced the exploration of the central area and tended to spend more time in the periphery, which was presented as enhanced thigmotaxis, suggesting adult *brsk2b*^{-/-} zebrafish also exhibited a more anxious state.

Although phenotyping and genotyping assessments of patients implicate damaging variants in *BRSK2* as contributing to autism, sufficient evidence is lacking to further verify the correlation between *BRSK2* and ASD and its underlying molecular mechanism based on animal models. To fill in this gap, we conducted several behavioral tests to evaluate whether *brsk2b* mutant zebrafish exhibit ASD-like features. The results showed that *brsk2b*^{-/-} zebrafish exhibited significant aberrant behavior compared to *brsk2b*^{+/+} zebrafish. In both juveniles and adults, in the social preference test, *brsk2b*^{-/-} zebrafish exhibited social impairment as some of their preference to conspecifics reduced significantly compared to *brsk2b*^{+/+} fish. In addition, *brsk2b* mutant zebrafish swam loosely in a group, while *brsk2b*^{+/+} zebrafish aggregated with each other, indicating that *brsk2b* dysfunction impacted the sociality of *brsk2b* mutant fish. Moreover, *brsk2b* mutant zebrafish tended to swim in stereotyped behavioral patterns such as “circling” and “walling” in the open field test, although there was no statistically significant difference compared to wild-type zebrafish. In conclusion, *brsk2b* mutant zebrafish displayed ASD-like behaviors.

To further understand the underlying molecular mechanisms of alterations in the morphology and behavior of *brsk2b*-deficient zebrafish, we detected the mRNA expression level of genes related to neurogenesis. The results showed that the expression levels of *homer1b*, *mbpa*, *mpz*, and *plp1b* in *brsk2b*^{-/-} zebrafish were significantly increased while the *isl1a* distinctly decreased. Human HOMER1 is a postsynaptic density scaffolding protein that is highly expressed in the hippocampus, corpus striatum, and cortex, which regulates the morphogenesis of synapses and dendritic spines (Yoon et al., 2021). The up-regulated expression of *homer1b* in *brsk2b*^{-/-} zebrafish indicates that these processes relevant to synaptogenesis may be disrupted. ISL1 is restricted in the motor neurons and is required for various phases of motor neuron development (Kim et al., 2015). *Isl1* mutant mice manifest motor function disabilities and have impaired axonal trajectories and axon specifications for motor neurons (Liang et al., 2011). As *BRSK* kinases were also identified as regulating synapse maturation at neuromuscular junctions (Lilley et al., 2014), we speculate that *brsk2b* might correspond to *isl1a* in motor neuron function; thus, *brsk2b* deficiency led to the disabled locomotor function of *brsk2b* mutant zebrafish. Further research on the roles of *isl1* in *brsk2*-affected motor function would be helpful to elucidate the mechanism of motor disorder in *BRSK2* patients. The

human MBP protein is a critical component of myelin (Herbert et al., 2017), and *MPZ* is expressed exclusively in Schwann cells. Mutations in *MPZ* were associated with the peripheral neuropathy Charcot-Marie-Tooth disease type 1 (Sanmaneechai et al., 2015). The *PLP1* gene plays a critical role in oligodendrocyte development and myelin sheath formation by promoting sheath compaction (Nobuta et al., 2019). Actually, large previous studies have linked oligodendrocyte dysfunction with ASD (Galvez-Contreras et al., 2020). Magnetic resonance imaging detected myelination defects and an abnormal morphology of white matter in ASD patients (Deoni Zinkstok et al., Deoni Zinkstok et al.; Aoki et al., 2017). Similarly, animal models of ASD displayed myelination dysfunction and disturbed regulation of oligodendrocyte-specific genes (Kawamura et al., 2020; Phan et al., 2020). Altogether, the expression changes of these genes indicate that *brsk2* deficiency may disturb the processes of oligodendrocytes maturation and myelin sheath formation and lead to morphological and behavioral abnormalities that are relevant to neurological disorders and ASD.

Since the *BRSK2* gene is duplicated as *brsk2a* and *brsk2b* in zebrafish and these genes have highly conserved amino acid sequences, we speculate that *brsk2a* plays a parallel role to *brsk2b*, thus it may compensate for the function of *brsk2b* when it is mutated. Therefore, a *brsk2a* and *brsk2b* double mutant zebrafish model is necessary to provide further support to the correlation between *BRSK2* and ASD occurrence. In particular, our research preliminarily found that *brsk2b* deficiency affected oligodendrocyte and synaptic structure-related genes. Therefore, in future studies, the function of oligodendrocyte lineage cells and molecular pathways relevant to synaptogenesis involved in *BRSK2* and autism should be examined based on a *brsk2a/brsk2b* double mutant zebrafish model, hoping to find new approaches and potential drugs for the treatment of ASD.

In this study, we identified a proband with a *de novo* non-sense variant in *BRSK2* (p.R222X) exhibiting typical ASD behaviors. For the first time, this work provided a new genetic model of *brsk2b* mutant zebrafish, which displayed impaired social preferences and disturbed shoaling behaviors as well as distinct locomotor defects. The increased expression level of *homer1b*, *mbpa*, *mpz*, and *plp1b* suggests that these ASD-like phenotypes may be involved in postsynaptic structure and oligodendrocyte and myelin sheath function, which remain to be further studied in future work.

DATA AVAILABILITY STATEMENT

The original contributions presented in the study are included in the article/**Supplementary Material**, further inquiries can be directed to the corresponding authors.

ETHICS STATEMENT

The studies involving human participants were reviewed and approved by the Research Ethics Board of Children’s Hospital of Fudan University. Written informed consent to participate in this

study was provided by the participants' legal guardian/next of kin. The animal study was reviewed and approved by the Research Ethics Board of Children's Hospital of Fudan University.

AUTHOR CONTRIBUTIONS

CL and XX conceived and supervised the study. XX, CL, and JD designed the experiments. JD performed the experiments and analyzed the data. JD, YW, and MH provided homozygous identification. QL and JL provided technical assistance in behavioral tests. JD and CL wrote the manuscript. All authors contributed to the article and approved the submitted version.

FUNDING

This work was supported by funds from the National Natural Science Foundation of China (NSFC, No. 82171540) and "Haiju" International Joint Laboratory of National Children's Medical Center of Children's Hospital of Fudan University (No. EK1125180106) to XX. This study was also supported by grants from the National Natural Science Foundation of China (NSFC,

No. 82101945) and Clinical Research of Shanghai Municipal Health Commission (No. 20204Y0102) to CL.

ACKNOWLEDGMENTS

We are grateful to all members of the Division of Child Health Care and Center for Translational Medicine of Children's Hospital of Fudan University in China. We thank Mu Yu (Institute of Neuroscience and State Key Laboratory of Neuroscience, Shanghai Institutes for Biological Sciences, Chinese Academy of Sciences, 320 Yue-Yang Road, Shanghai 200031, China) for the guidance on the experiments and Xu Wang (Institute of Metabolism and Integrative Biology, Fudan University, Shanghai 200438, China) for providing the Tg (*HuC*: RFP) transgenic line.

SUPPLEMENTARY MATERIAL

The Supplementary Material for this article can be found online at: <https://www.frontiersin.org/articles/10.3389/fnmol.2022.904935/full#supplementary-material>

REFERENCES

- Albadri, S., De Santis, F., Di Donato, V., and Del Bene, F. (2017). "CRISPR/Cas9-Mediated Knockin and Knockout in Zebrafish," in *Genome Editing in Neurosciences*, eds R. Jaenisch, F. Zhang, and F. Gage (Cham: Springer), 41–49.
- Aoki, Y., Yoncheva, Y. N., Chen, B., Nath, T., Sharp, D., Lazar, M., et al. (2017). Association of White Matter Structure With Autism Spectrum Disorder and Attention-Deficit/Hyperactivity Disorder. *JAMA Psychiatry* 74, 1120–1128. doi: 10.1001/jamapsychiatry.2017.2573
- Auer, T. O., Duroure, K., De Cian, A., Concordet, J. P., and Del Bene, F. (2014). Highly efficient CRISPR/Cas9-mediated knock-in in zebrafish by homology-independent DNA repair. *Genome Res.* 24, 142–153. doi: 10.1101/gr.161638.113
- Bai, D., Yip, B. H. K., Windham, G. C., Sourander, A., Francis, R., Yoffe, R., et al. (2019). Association of Genetic and Environmental Factors With Autism in a 5-Country Cohort. *JAMA Psychiatry* 76, 1035–1043. doi: 10.1001/jamapsychiatry.2019.1411
- Barnes, A. P., Lilley, B. N., Pan, Y. A., Plummer, L. J., Powell, A. W., Raines, A. N., et al. (2007). LKB1 and SAD kinases define a pathway required for the polarization of cortical neurons. *Cell* 129, 549–563. doi: 10.1016/j.cell.2007.03.025
- Basnet, R. M., Zizioli, D., Taweedit, S., Finazzi, D., and Memo, M. (2019). Zebrafish Larvae as a Behavioral Model in Neuropharmacology. *Biomedicines* 7:23. doi: 10.3390/biomedicines7010023
- Burton, C. E., Zhou, Y., Bai, Q., and Burton, E. A. (2017). Spectral properties of the zebrafish visual motor response. *Neurosci. Lett.* 646, 62–67. doi: 10.1016/j.neulet.2017.03.002
- Castelbaum, L., Sylvester, C. M., Zhang, Y., Yu, Q., and Constantino, J. N. (2020). On the Nature of Monozygotic Twin Concordance and Discordance for Autistic Trait Severity: A Quantitative Analysis. *Behav. Genet.* 50, 263–272. doi: 10.1007/s10519-019-09987-2
- Colón-Rodríguez, A., Uribe-Salazar, J. M., Weyenberg, K. B., Sriram, A., Quezada, A., Kaya, G., et al. (2020). Assessment of Autism Zebrafish Mutant Models Using a High-Throughput Larval Phenotyping Platform. *Front. Cell. Dev. Biol.* 8:586296. doi: 10.3389/fcell.2020.586296
- Deoni, S. C., Zinkstok, J. R., Daly, E., Ecker, C., Williams, S. C., and Murphy, D. G. (2015). White-matter relaxation time and myelin water fraction differences in young adults with autism. *Psychol. Med.* 45, 795–805. doi: 10.1017/S0033291714001858
- Dhumale, P., Menon, S., Chiang, J., and Puschel, A. W. (2018). The loss of the kinases SadA and SadB results in early neuronal apoptosis and a reduced number of progenitors. *PLoS One* 13:e0196698. doi: 10.1371/journal.pone.0196698
- Ellis, L. D., Seibert, J., and Soanes, K. H. (2012). Distinct models of induced hyperactivity in zebrafish larvae. *Brain Res.* 1449, 46–59. doi: 10.1016/j.brainres.2012.02.022
- Feliciano, P., Zhou, X., Astrovskaya, I., Turner, T. N., Wang, T., Brueggeman, L., et al. (2019). Exome sequencing of 457 autism families recruited online provides evidence for autism risk genes. *NPJ Genom. Med.* 4:19. doi: 10.1038/s41525-019-0093-8
- Galvez-Contreras, A. Y., Zarate-Lopez, D., Torres-Chavez, A. L., and Gonzalez-Perez, O. (2020). Role of Oligodendrocytes and Myelin in the Pathophysiology of Autism Spectrum Disorder. *Brain Sci.* 10:951. doi: 10.3390/brainsci10120951
- Geng, Y., and Peterson, R. T. (2019). The zebrafish subcortical social brain as a model for studying social behavior disorders. *Dis. Model Mech.* 12:dmm039446. doi: 10.1242/dmm.039446
- Grillner, S., and El Manira, A. (2020). Current Principles of Motor Control, with Special Reference to Vertebrate Locomotion. *Physiol. Rev.* 100, 271–320. doi: 10.1152/physrev.00015.2019
- Hansen, S. N., Schendel, D. E., Francis, R. W., Windham, G. C., Bresnahan, M., Levine, S. Z., et al. (2019). Recurrence Risk of Autism in Siblings and Cousins: A Multinational, Population-Based Study. *J. Am. Acad. Child Adolesc. Psychiatry* 58, 866–875. doi: 10.1016/j.jaac.2018.11.017
- Herbert, A. L., Fu, M. M., Drerup, C. M., Gray, R. S., Harty, B. L., Ackerman, S. D., et al. (2017). Dynein/dynactin is necessary for anterograde transport of Mbp mRNA in oligodendrocytes and for myelination in vivo. *Proc. Natl. Acad. Sci. U S A.* 114, E9153–E9162. doi: 10.1073/pnas.1711088114
- Hiatt, S. M., Thompson, M. L., Prokop, J. W., Lawlor, J. M. J., Gray, D. E., Bebin, E. M., et al. (2019). Deleterious Variation in BRSK2 Associates with a Neurodevelopmental Disorder. *Am. J. Hum. Genet.* 104, 701–708. doi: 10.1016/j.ajhg.2019.02.002
- Kalueff, A. V., Gebhardt, M., Stewart, A. M., Cachat, J. M., Brimmer, M., Chawla, J. S., et al. (2013). Towards a comprehensive catalog of zebrafish behavior 1.0 and beyond. *Zebrafish* 10, 70–86. doi: 10.1089/zeb.2012.0861

- Kaminsky, E. B., Kaul, V., Paschall, J., Church, D. M., Bunke, B., Kunig, D., et al. (2011). An evidence-based approach to establish the functional and clinical significance of copy number variants in intellectual and developmental disabilities. *Genet. Med.* 13, 777–784. doi: 10.1097/GIM.0b013e31822c79f9
- Kawamura, A., Katayama, Y., Nishiyama, M., Shoji, H., Tokuoka, K., Ueta, Y., et al. (2020). Oligodendrocyte dysfunction due to Chd8 mutation gives rise to behavioral deficits in mice. *Hum. Mol. Genet.* 29, 1274–1291. doi: 10.1093/hmg/ddaa036
- Kim, N., Park, C., Jeong, Y., and Song, M. R. (2015). Functional Diversification of Motor Neuron-specific Isl1 Enhancers during Evolution. *PLoS Genet.* 11:e1005560. doi: 10.1371/journal.pgen.1005560
- Kishi, M., Pan, Y. A., Crump, J. G., and Sanes, J. R. (2005). Mammalian SAD kinases are required for neuronal polarization. *Science* 307, 929–932. doi: 10.1126/science.1107403
- Krylov, V. V., Izvekoev, E. I., Pavlova, V. V., Pankova, N. A., and Osipova, E. A. (2021). Circadian rhythms in zebrafish (*Danio rerio*) behaviour and the sources of their variability. *Biol. Rev. Camb. Philos. Soc.* 96, 785–797. doi: 10.1111/brv.12678
- Liang, X., Song, M. R., Xu, Z., Lanuza, G. M., Liu, Y., Zhuang, T., et al. (2011). Isl1 is required for multiple aspects of motor neuron development. *Mol. Cell Neurosci.* 47, 215–222. doi: 10.1016/j.mcn.2011.04.007
- Lilley, B. N., Krishnaswamy, A., Wang, Z., Kishi, M., Frank, E., and Sanes, J. R. (2014). SAD kinases control the maturation of nerve terminals in the mammalian peripheral and central nervous systems. *Proc. Natl. Acad. Sci. U S A.* 111, 1138–1143. doi: 10.1073/pnas.1321990111
- Liu, C. X., Li, C. Y., Hu, C. C., Wang, Y., Lin, J., Jiang, Y. H., et al. (2018). CRISPR/Cas9-induced shank3b mutant zebrafish display autism-like behaviors. *Mol. Autism* 9:23. doi: 10.1186/s13229-018-0204-x
- Liu, Y., Wang, Y., Li, N., and Jiang, S. (2022). Avobenzone and nanoplastics affect the development of zebrafish nervous system and retinal system and inhibit their locomotor behavior. *Sci. Total Environ.* 806:150681. doi: 10.1016/j.scitotenv.2021.150681
- Lord, C., Brugha, T. S., Charman, T., Cusack, J., Dumas, G., Frazier, T., et al. (2020). Autism spectrum disorder. *Nat. Rev. Dis. Primers* 6:5. doi: 10.1038/s41572-019-0138-4
- Mahabir, S., Chatterjee, D., Buske, C., and Gerlai, R. (2013). Maturation of shoaling in two zebrafish strains: a behavioral and neurochemical analysis. *Behav. Brain Res.* 247, 1–8. doi: 10.1016/j.bbr.2013.03.013
- Meshalkina, D. A., Kizlyk, M. N., Kysil, E. V., Collier, A. D., Echevarria, D. J., Abreu, M. S., et al. (2018). Zebrafish models of autism spectrum disorder. *Exp. Neurol.* 299, 207–216. doi: 10.1016/j.expneurol.2017.02.004
- Miller, D. T., Adam, M. P., Aradhya, S., Biesecker, L. G., Brothman, A. R., Carter, N. P., et al. (2010). Consensus statement: chromosomal microarray is a first-tier clinical diagnostic test for individuals with developmental disabilities or congenital anomalies. *Am. J. Hum. Genet.* 86, 749–764. doi: 10.1016/j.ajhg.2010.04.006
- Muller, M., Lutter, D., and Puschel, A. W. (2010). Persistence of the cell-cycle checkpoint kinase Wee1 in SadA- and SadB-deficient neurons disrupts neuronal polarity. *J. Cell Sci.* 123, 286–294. doi: 10.1242/jcs.058230
- Nakanishi, K., Niida, H., Tabata, H., Ito, T., Hori, Y., Hattori, M., et al. (2019). Isozyme-Specific Role of SAD-A in Neuronal Migration During Development of Cerebral Cortex. *Cereb. Cortex* 29, 3738–3751. doi: 10.1093/cercor/bhy253
- Nie, J., Liu, X., Lilley, B. N., Zhang, H., Pan, Y. A., Kimball, S. R., et al. (2013). SAD-A kinase controls islet beta-cell size and function as a mediator of mTORC1 signaling. *Proc. Natl. Acad. Sci. U S A.* 110, 13857–13862. doi: 10.1073/pnas.1307698110
- Nobuta, H., Yang, N., Ng, Y. H., Marro, S. G., Sabeur, K., Chavali, M., et al. (2019). Oligodendrocyte Death in Pelizaeus-Merzbacher Disease Is Rescued by Iron Chelation. *Cell Stem Cell* 25, 531–541.e6. doi: 10.1016/j.stem.2019.09.003
- Peng, X., Lin, J., Zhu, Y., Liu, X., Zhang, Y., Ji, Y., et al. (2016). Anxiety-related behavioral responses of pentylentetrazole-treated zebrafish larvae to light-dark transitions. *Pharmacol. Biochem. Behav.* 145, 55–65. doi: 10.1016/j.pbb.2016.03.010
- Phan, B. N., Bohlen, J. F., Davis, B. A., Ye, Z., Chen, H. Y., Mayfield, B., et al. (2020). A myelin-related transcriptomic profile is shared by Pitt-Hopkins syndrome models and human autism spectrum disorder. *Nat. Neurosci.* 23, 375–385. doi: 10.1038/s41593-019-0578-x
- Rea, V., and Van Raay, T. J. (2020). Using Zebrafish to Model Autism Spectrum Disorder: A Comparison of ASD Risk Genes Between Zebrafish and Their Mammalian Counterparts. *Front. Mol. Neurosci.* 13:575575. doi: 10.3389/fnmol.2020.575575
- Ronemus, M., Iossifov, I., Levy, D., and Wigler, M. (2014). The role of de novo mutations in the genetics of autism spectrum disorders. *Nat. Rev. Genet.* 15, 133–141. doi: 10.1038/nrg3585
- Ruzzo, E. K., Perez-Cano, L., Jung, J. Y., Wang, L. K., Kashef-Haghighi, D., Hartl, C., et al. (2019). Inherited and De Novo Genetic Risk for Autism Impacts Shared Networks. *Cell* 178, 850–866.e26. doi: 10.1016/j.cell.2019.07.015
- Sakai, C., Ijaz, S., and Hoffman, E. J. (2018). Zebrafish Models of Neurodevelopmental Disorders: Past, Present, and Future. *Front. Mol. Neurosci.* 11:294. doi: 10.3389/fnmol.2018.00294
- Sanmaneechai, O., Feely, S., Scherer, S. S., Herrmann, D. N., Burns, J., Muntoni, F., et al. (2015). Genotype-phenotype characteristics and baseline natural history of heritable neuropathies caused by mutations in the MPZ gene. *Brain* 138, 3180–3192. doi: 10.1093/brain/awv241
- Satterstrom, F. K., Kosmicki, J. A., Wang, J., Breen, M. S., De Rubeis, S., An, J. Y., et al. (2020). Large-Scale Exome Sequencing Study Implicates Both Developmental and Functional Changes in the Neurobiology of Autism. *Cell* 180, 568–584.e23. doi: 10.1016/j.cell.2019.12.036
- Schnorr, S. J., Steenbergen, P. J., Richardson, M. K., and Champagne, D. L. (2012). Measuring thigmotaxis in larval zebrafish. *Behav. Brain Res.* 228, 367–374. doi: 10.1016/j.bbr.2011.12.016
- Sharma, S., Coombs, S., Patton, P., and Burt de Perera, T. (2009). The function of wall-following behaviors in the Mexican blind cavefish and a sighted relative, the Mexican tetra (*Astyanax*). *J. Comp. Physiol. A. Neuroethol. Sens. Neural. Behav. Physiol.* 195, 225–240. doi: 10.1007/s00359-008-0400-9
- Tick, B., Bolton, P., Happe, F., Rutter, M., and Rijdsdijk, F. (2016). Heritability of autism spectrum disorders: a meta-analysis of twin studies. *J. Child Psychol. Psychiatry* 57, 585–595. doi: 10.1111/jcpp.12499
- Treit, D., and Fundytus, M. (1988). Thigmotaxis as a test for anxiolytic activity in rats. *Pharmacol. Biochem. Behav.* 31, 959–962. doi: 10.1016/0091-3057(88)90413-3
- Yoon, S., Piguel, N. H., Khalatyan, N., Dionisio, L. E., Savas, J. N., and Penzes, P. (2021). Homer1 promotes dendritic spine growth through ankyrin-G and its loss reshapes the synaptic proteome. *Mol. Psychiatry* 26, 1775–1789. doi: 10.1038/s41380-020-00991-1

Conflict of Interest: The authors declare that the research was conducted in the absence of any commercial or financial relationships that could be construed as a potential conflict of interest.

Publisher's Note: All claims expressed in this article are solely those of the authors and do not necessarily represent those of their affiliated organizations, or those of the publisher, the editors and the reviewers. Any product that may be evaluated in this article, or claim that may be made by its manufacturer, is not guaranteed or endorsed by the publisher.

Copyright © 2022 Deng, Wang, Hu, Lin, Li, Liu and Xu. This is an open-access article distributed under the terms of the Creative Commons Attribution License (CC BY). The use, distribution or reproduction in other forums is permitted, provided the original author(s) and the copyright owner(s) are credited and that the original publication in this journal is cited, in accordance with accepted academic practice. No use, distribution or reproduction is permitted which does not comply with these terms.